

Kink-Antikink Collisions in the Periodic φ^4 Model

M. Mohammadi^{1*}
 physmohammadi@pgu.ac.ir

R. Dehghani²
 r.dehghani@queensu.ca

¹*Physics Department, Persian Gulf University, Bushehr 75169, Iran.*

²*Department of Physics, Engineering Physics & Astronomy Stirling Hall, Queen's University 64 Bader Lane Kingston, Ontario, Canada.*

Abstract

We borrow the form of potential of the well-known kink-bearing φ^4 system in the range between its two vacua and paste it repeatedly into the other ranges to introduce the periodic φ^4 system. The paper is devoted to providing a comparative numerical study of the properties of the two systems. Although the two systems are quite similar for a kink (antikink) solution, they usually exhibit different behaviors throughout collisions. For instance, they have different critical velocities, different results during collisions, and a different rule in their quasi-fractal structures. Their quasi-fractal structures will be studied in the disturbed kink-antikink collisions as well. Hence, three types of scattering windows will be introduced with respect to the incoming speed, the amplitude, and initial phase of the internal mode, respectively. Moreover, a detailed comparative study of the collisions between two kinks and one antikink will be done at the end.

Keywords : periodic φ^4 , kink, soliton, fractal.

1 Introduction

Nonlinear field models with topological kink (antikink) solutions in $1 + 1$ dimensions are of growing interest for theoretical physics from high energy physics and cosmology to condensed matter physics [1–13]. Especially in cosmology, the structure and dynamics of domain walls, can be modeled or described by the $(1+1)$ -dimensional kink-bearing theories [9–15]. Topological kink (-like) solutions also exist in more complex models with two or more fields in $(1+1)$ -dimensions [16–28]. Complex kink (antikink) solution is another type of topological soliton-like solutions which was obtained for a complex nonlinear Klein-Gordon field system [29].

The dynamic and other properties of kinks have been of great importance and have attracted the attention of physicists and mathematicians for a long time [30–89]. In particular, the kink-(anti)kink scattering and the interactions of kinks with impurities were actively studied previously [48–56]. In this context, the recent interesting results on kink-antikink interactions in models, which possess kinks with power-law tails, can be mentioned [57–62]. It is also worth mentioning that the recent results on the study of maximal values of different quantities in multi-soliton (kink and antikink) collisions have been another topic of interest to researchers in recent years [63–65]. There have been different methods to study the behaviours of kinks (antikinks) in the interactions among which one can mention the quasi-exact numerical methods, and the approximate methods such as the collective coordinate approximation [41, 66–71] and the Manton's method [71–73]. However, in this paper, we only use a numerical method to obtain the results.

*Corresponding Author.

For some kink solutions, there is an ability to keep a constant oscillatory internal motion with a specific frequency. This phenomenon is related to whether there is a non-trivial internal mode for the kink (antikink) solution [74–76]. Internal modes are the bound states of a Schrödinger-like equation which was obtained by considering the small fluctuations on a kink solution. Kink-bearing systems, depending on whether they have non-trivial internal modes, can be divided into nearly integrable and non-integrable models [76–78]. In this context the only integrable model is the well-known sine-Gordon (SG) system. It was shown that the energy loss due to the radiation during the collision is usually small in the nearly integrable models in comparison with non-integrable models. The amount of radiation is a complicated function of the initial speed, and depending on that, the fate of a kink-antikink collision can be completely different. In general, the collision between a kink and an antikink may lead to a long-living non-topological oscillating bound state, so called a bion state, or they may eventually bounce back and reflect from each other, or they may annihilate immediately in radiative systems [79].

For any kink-bearing system except the SG system, there is always a critical speed v_{cr} for which if the initial speed v_{in} of a head-on kink-antikink collision is greater, kink and antikink pass through one another and reappear after collisions with a constantly vibrational behavior. If the initial incoming speed v_{in} is smaller than the critical speed v_{cr} ($v_{in} < v_{cr}$), the kink and antikink usually form a bion state that decays slowly and radiates energy in the form of small-amplitude waves. In a number of models, when $v_{in} < v_{cr}$, there have been spotted a new interesting phenomenon called the escape or scattering windows. For such initial speeds, because of the resonance energy exchange between the translational and vibrational internal modes, the two kinks (antikinks) will not form a bion and will bounce off each other after two or more collisions [31, 36, 80, 81]. Moreover, a prominent feature of such systems is the appearance of a chaotic quasi-fractal structure with a hierarchical order of scattering windows [75, 82–84].

In this regard, the φ^4 model which is a well-known kink-bearing system, was studied extensively, namely, in relation to the resonant kink-antikink scattering and the quasi-fractal structure [31, 75, 82], kinks interaction with impurities [51–53, 56], high energy density in the collision of N solitons [64], ac external force [85], scattering between wobbling kinks [86], and the periodically modulated on-site potential [87]. The corresponding potential of the φ^4 system is as follows:

$$V(\varphi) = \frac{1}{2}(\varphi^2 - 1)^2, \quad (1)$$

It has a single non-trivial internal mode $\psi(x) \propto \tanh(x) \operatorname{sech}(x)$ with a specific rest frequency $\omega_o = \sqrt{3}$ [31, 75]. In this paper, inspired by the well-known φ^4 model, a new kink-bearing system can be introduced that can be called the periodic φ^4 model with following form of the potential [88]:

$$V(\varphi) = \frac{1}{2}((\varphi - 2N)^2 - 1)^2, \quad 2N - 1 \leq \varphi < 2N + 1, \quad (2)$$

where $N = 0, \pm 1, \pm 2, \dots$. The potential of the new system is the same as that of the φ^4 system in the range $-1 < \varphi < 1$, which is repeated in other regions of the real scalar field φ (see Fig. 1). Although both systems have the same form of potential in the range $-1 \leq \varphi \leq 1$ and have identical soliton (kink and antikink) solutions, they exhibit different behaviors in the collisions (interactions) due to their differences elsewhere (i.e. $\varphi < -1$ and $1 < \varphi$). From a physical point of view, this is important because it attracts attention to fact that the similarity of particles may not necessarily mean that their interaction is the same. In other words, comparing these two particular models, just as an example, indicates the possibility that there may be similar particles in the nature that exhibit different interaction behaviors. The main purpose of this paper is to present a comparative study of the interaction properties of these systems. Accordingly,

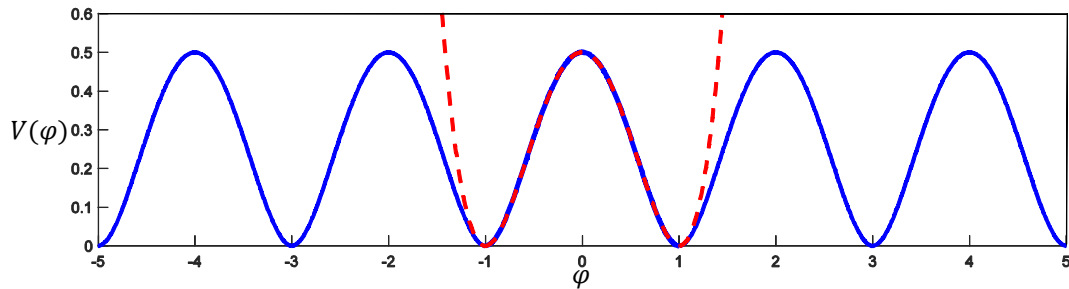


Figure 1: The red dash (solid blue) curve is representing the potential of the (periodic) φ^4 model. In fact we copy the potential of the φ^4 model in the range from -1 to 1 and paste it in multiple regions such as -1 to -3 , -3 to -5 , 1 to 3 , 3 to 5 , and so on, to introduce the potential of the periodic φ^4 system.

the collisions, the scattering windows, and the quasi-fractal structure of both systems will be investigated and compared in detail.

Our paper is organized as follows. In section 2, we review, briefly, the formulation and some general properties of a relativistic kink-bearing system in $1+1$ dimensions. Also, the necessary numerical considerations for the obtained results are presented in this section. In Section 3, the internal modes of the kink (antikink) solutions are considered in detail. Section 4 is devoted to all numerical results, which have been obtained for both φ^4 and periodic φ^4 systems. The last section is devoted to summary and conclusions, where we also formulate some possible directions for further research.

2 Basic Equations

In general, the Lagrangian density of a kink-bearing system in $1+1$ dimensions is

$$\mathcal{L} = \frac{1}{2} \left(\frac{\partial \varphi}{\partial t} \right)^2 - \frac{1}{2} \left(\frac{\partial \varphi}{\partial x} \right)^2 - V(\varphi), \quad (3)$$

where φ is a real scalar field and the self-interaction term $V(\varphi)$ is called the potential. Using the Euler-Lagrange equation, the equation of motion can be derived as:

$$\ddot{\varphi} - \varphi'' = -\frac{dV}{d\varphi}, \quad (4)$$

where $\ddot{\varphi}$ and φ'' are the second derivatives of the scalar field φ with respect to time and space, respectively. For the dynamical field equation (4), there are various manifestations of the potential $V(\varphi)$ that yield well-known kink (antikink) solutions. In fact, if the positive definite potential $V(\varphi)$ has at least two degenerate vacua (i.e. points of minimum potential), there will be localized solutions called kinks and antikinks with positive and negative topological charges, respectively. For the φ^4 model (1), there are only two degenerate minima (vacua), at -1 and 1 , thus, there is only one type of kink and antikink solution that belongs to a unique sector $(-1, 1)$ [30]. However, for the periodic φ^4 model (2), similar to the well-known sG model, there are infinite vacua, i.e. any odd number (see Fig. 1), hence there are infinite types of kink and antikink solutions belonging to infinite sectors $(2N-1, 2N+1)$.

In order to find a moving non-vibrational topological kink solution, we should consider the dynamical equation (4) for a solution in the following form: $\varphi_v = \varphi_o(\gamma(x - x_o - vt))$, where v is the velocity of the kink, $\gamma = 1/\sqrt{1-v^2}$ is the Lorentz factor, x_o is the initial position, and φ_o is an unknown function which should be found. If one does this procedure for the periodic φ^4 system (2), the moving non-vibrational kink and antikink solutions for sector $(2N-1, 2N+1)$, i.e. $2N-1 < \varphi < 2N+1$, will be

$$\varphi_v(x, t) = \tanh(\pm\gamma(x - x_o - vt)) + 2N, \quad (5)$$

where $+$ ($-$) is used for kinks (antikinks), and N is any integer number. Note that the above solutions for $N = 0$ are the same kink and antikink solutions of the ordinary φ^4 system.

For such a system, the superposition of two or multiple kinks and antikinks can be assumed as new solutions of the system, provided they are far enough from one another. For example, for m number of the solitary wave solutions (kinks and antikinks), which initially have different velocities v_i and initial positions x_i , the following combination

$$\varphi = \sum_{i=1}^m \tanh(\pm\gamma_i(x - v_i t - x_i)) + C, \quad x_{i+1} - x_i \gg 1, \quad (6)$$

where $\gamma_i = 1/\sqrt{1 - v_i^2}$, is again a solution of the system. Here, \pm means that for any solitary wave solution which initially stands at x_i , choosing $+$ (kink) or $-$ (antikink) is optional. The constant C is a proper number which should be included in order to have right boundary conditions. In fact, the relative distance between the kinks and antikinks are quite large to ensure that the overlap of the kinks and antikinks are negligibly small. It should be noted that, for the ordinary φ^4 system, since there are two vacuum points at -1 and $+1$, only the collisions of the alternative combinations of the kink and antikink solutions are possible to be studied. However, for the periodic φ^4 model there are no conditions on the initial arrangement of kinks and antikinks like the SG system.

In general, since it has not been possible to obtain multisolitonic solutions of the non-integrable systems analytically, it is common to use numerical methods to study the collisions of any number of kinks and antikinks. Using a superposition of several far apart kinks and antikinks, which are moving towards the collision point, is the necessary initial condition for a numerical investigation of the collisions. To acquire numerical results of the equation of motion (4), we use the discretized version of that in the following form [82]:

$$\frac{\partial^2 \varphi_n}{\partial t^2} - \frac{1}{h^2}(\varphi_{n-1} - 2\varphi_n + \varphi_{n+1}) + \frac{1}{12h^2}(\varphi_{n-2} - 4\varphi_{n-1} + 6\varphi_n - 4\varphi_{n+1} + \varphi_{n+2}) + \frac{dV(\varphi_n)}{d\varphi_n} = 0, \quad (7)$$

where V is represented either by Eq. (1) or Eq. (2), h is the small spatial step, $n = 0, \pm 1, \pm 2, \dots$ and $\varphi_n = \varphi(nh, t)$. A fourth-order Runge-Kutta scheme with the small time-step k is used to solve the ordinary differential equations (7) numerically. The accuracy of this standard method is to fourth order in both temporal and spatial steps. In this paper, all the simulations were carried out for $h = k = 0.02$. To avoid the reflective effects of boundaries on the accuracy of simulations, we fix them at far distances from the origin ($x = 0$), namely from -200 to 200 in this paper. It is also necessary to say that all simulations were done in the time interval $0 < t < 400$.

From the Noether's theorem, the energy functional corresponding to the Lagrangian (3) is viewed as:

$$E[\varphi] = \int_{-\infty}^{+\infty} \varepsilon(x, t) dx = \int_{-\infty}^{+\infty} \left(\frac{1}{2}\dot{\varphi}^2 + \frac{1}{2}\varphi'^2 + V(\varphi) \right) dx = K + U + P. \quad (8)$$

where

$$\varepsilon(x, t) = k(x, t) + u(x, t) + p(x, t), \quad (9)$$

is the energy density function and functions $k(x, t)$, $u(x, t)$, and $p(x, t)$ are introduced as

$$k(x, t) = \frac{1}{2} \left(\frac{\partial \varphi}{\partial t} \right)^2, \quad u(x, t) = \frac{1}{2} \left(\frac{\partial \varphi}{\partial x} \right)^2, \quad p(x, t) = V(\varphi) = \frac{1}{2}((\varphi - 2n)^2 - 1)^2 \quad (10)$$

Accordingly, the total energy of the system (8) can be written as the sum of three portions: the kinetic energy K , the gradient energy U , and the potential energy P , that are defined

as the integrations of the $k(x, t)$, $u(x, t)$, and $p(x, t)$, above the whole space, respectively. Hence, $k(x, t)$, $u(x, t)$, and $p(x, t)$ are called the kinetic, the gradient, and the potential energy density, respectively. The details of any collision can be more clarified by studying the evolution of all these parts throughout the collisions.

In the numerical calculations, we need to somehow be able to obtain the velocity of an entity after the collisions. To do that, we calculate the energy E (8) and the momentum P of this entity and simply use the relativistic relation $v = P/E$. The corresponding momentum for the Lagrangian density (3) would be:

$$P[\varphi] = \int_{-\infty}^{+\infty} (-\dot{\varphi}\varphi')dx, \quad (11)$$

that is another obvious result from the Noether's theorem as well as equation (8).

3 Internal modes

A kink (antikink) has the lowest energy among the other solutions with the same asymptotic behaviour [30, 89]. Therefore, we can expect that any permissible small deformation above a kink (antikink) solution, finally leads to an increase in the total energy. In general, a small deformed kink solution which is at rest, can be introduced as follows:

$$\phi_o(x, t) = \varphi_o(x) + \delta\varphi(x, t), \quad (12)$$

where $\varphi_o(x)$ is the same non-moving kink solution (for example Eq. (5) for $v = 0$) and $\delta\varphi(x, t)$ is any permissible small function. Note that a permissible deformation $\delta\varphi(x, t)$ is one for which $\phi_o(x, t)$ is again a solution of the equations of motion (4). In other words, for a non-moving kink (antikink) solution which is slightly deformed (12), we expect:

$$\square(\varphi_o + \delta\varphi) = (\delta\ddot{\varphi}) - (\varphi_o'' + \delta\varphi'') = -\frac{dV(\varphi_o + \delta\varphi)}{d(\varphi_o + \delta\varphi)}, \quad (13)$$

note that $\ddot{\varphi}_o = 0$. From Eq. (4), for a non-moving kink solution we have: $\varphi_o'' = \frac{dV(\varphi_o)}{d\varphi_o}$. Therefore, expanding to the first order in $\delta\varphi$, Eq. (13) simplifies to

$$\square(\delta\varphi) = \delta\ddot{\varphi} - \delta\varphi'' \approx -\mathcal{U}(x)\delta\varphi, \quad (14)$$

where $\mathcal{U}(x) = \frac{d^2U(\varphi_o)}{d\varphi_o^2}$ can be called the *kink potential*, it is also called *stability potential* or *quantum-mechanical potential*. Equation (14) can be considered as the dominant dynamical equation for the small permissible deformations $\delta\varphi$. Since Eq. (14) is a linear homogenous partial differential equation, we can solve it using variables separation method. Hence, one can consider a solution of the form $\delta\varphi(x, t) = \psi(x)\chi(t)$, provided $\psi(\pm\infty) = 0$, and substitute back into Eq. (14). Finally, it leads to two independent ordinary differential equations:

$$\ddot{\chi} = -\omega_o^2\chi, \quad (15)$$

$$-\psi'' + \mathcal{U}(x)\psi = \omega_o^2\psi, \quad (16)$$

where ω_o^2 is the constant of separation. The trivial independent solutions of Eq. (15) are $\cos(\omega_o t)$ and $\sin(\omega_o t)$, respectively. Equation (16) is a Schrödinger-like equation for which there are two different types of solutions which are called internal modes (bound states) and free modes. Internal modes (free modes) are some discrete (continuous) solutions of Eq. (16) for which $\omega_o^2 < \mathcal{U}(\pm\infty) = \mathcal{U}_f$ ($\omega_o^2 > \mathcal{U}(\pm\infty) = \mathcal{U}_f$) and exponentially (periodically) tend to zero ($\sin(\sqrt{\omega_o^2 - \mathcal{U}_f} x)$ or $\cos(\sqrt{\omega_o^2 - \mathcal{U}_f} x)$) at large distances.

In general, Eq. (16) always has a trivial solution $\psi = \xi \frac{d\varphi_o}{dx}$ with $\omega_o = 0$, where ξ is arbitrary provided that $|\psi| \ll 1$. However, this trivial solution is associated only with an

infinitesimal translation of the static kink (antikink)-solution [32, 33, 75], it has no other physical meaning. It has been seen numerically that the kink solutions, which have non-trivial bound states (internal modes), can keep a constantly oscillating behaviour after collisions (something similar to what is seen in Figs. 4 and 5). For example, for the φ^4 (periodic φ^4) system, which was introduced in the previous section, the related kink potential is $\mathcal{U}(x) = 4 - 6 \operatorname{sech}^2(x)$ for which there is a non-trivial bound state (internal mode) corresponding to $\omega_o^2 = 3$ and $\psi \propto \tanh(x) \operatorname{sech}(x)$ [32, 75]. The other systems, which have no non-trivial bound states, can never maintain a constantly oscillating behaviour after the collisions [23, 33, 78]. In fact, any non-trivial internal mode can be considered as a channel to impose an additional fluctuation on the kink (antikink) solution. To put it differently, it is a channel for kink (antikink) solution to absorb some external energies.

Relativistically speaking, if we know the exact space-time function of a scalar field in the rest frame, using a boost, we can get the corresponding space-time function in other inertial frames as follows: $t \rightarrow \gamma(t - vx)$ and $x \rightarrow \gamma(x - vt)$. For example, based on pervious discussions, if one considers a kink solution of both φ^4 and periodic φ^4 systems, the general disturbed version of that at rest can be introduced in the following form:

$$\phi_o(x, t) = \varphi_o(x) + \psi(x) \sin(\omega_o t + \theta_o), \quad (17)$$

where $\omega_o^2 = 3$, $\psi(x) = \xi \tanh(x) \operatorname{sech}(x)$ is the single non-trivial bound state of Eq. (16), and θ_o is an arbitrary initial phase. Therefore, the moving version of this disturbed kink (antikink) solution can be obtained easily:

$$\phi_v(x, t) = \phi_o(\gamma(x - vt), \gamma(t - vx)) = \varphi_o(\gamma(x - vt)) + \psi(\gamma(x - vt)) \sin(\omega_o \gamma(t - vx) + \theta_o). \quad (18)$$

by introducing $\omega = \omega_o \gamma$ and $k = \omega_o \gamma v$, we can simplify Eq. (18) to

$$\phi_v(x, t) = \varphi_v(x, t) + \psi(\gamma(x - vt)) \sin(\omega t - kx + \theta_o), \quad (19)$$

where $\varphi_v(x, t) = \varphi_o(\gamma(x - vt))$ is the same moving undisturbed kink (antikink) solution.

4 Collisions

In this section, we mainly focus on the results of the collisions between a kink and an antikink of both systems and compare them with one another. We set the conditions such as initial positions and velocities so that the kink and the antikink simultaneously arrive at a special point in space (i.e. $x = 0$) and collide. The relative distance between the kink and antikink is quite large to ensure that the overlap of the kink and antikink is negligibly small. For a comparative study between the two systems, the initial and boundary conditions must be the same for both. Hence, since two systems have the same potential in the range $-1 \leq \varphi \leq 1$, the combination of the initial kinks and anti-kinks, that their collision we are going to study, should be in such a way that the initial field φ is between -1 and 1 .

4.1 Primary Results

In a kink-antikink collision, due to the symmetrical potential of the φ^4 (periodic φ^4) model, there are no differences between the results of different orientations such as kink-antikink ($K\bar{K}$) and antikink-kink ($\bar{K}K$). The initial condition for this collision in the φ^4 (periodic φ^4) model is:

$$\varphi_{K\bar{K}} = \tanh(+\gamma(x - vt - a)) + \tanh(-\gamma(x + vt - b)) - 1, \quad (20)$$

where $a = -20$ and $b = 20$ are the initial positions, and v is the incoming speed. In the case of a kink-antikink collision, there is a critical speed which separates two regions of incoming speeds. For speeds less than the critical speed, kink and antikink usually

stick together and generate a bion state. For the φ^4 system, the critical speed is about $v_{cr} = 0.2600$, and for the periodic φ^4 we have found v_{cr} to be about 0.1516. This difference arises from the potential differences in the ranges $\varphi < -1$ and $\varphi > 1$. In other words, although two systems have the same kink and antikink solutions, their differences in the interaction region, i.e. $\varphi < -1$ and $\varphi > 1$, cause different critical speeds.

A bion is a long-living bound state with zero topological charge, which decays slowly via emitting its energy in the form of small amplitude waves. Figure 2 (3) shows some details of a $K\bar{K}$ collision at the same initial speed $v = 0.1$ below its critical speed in the context of the φ^4 (periodic φ^4) system, which finally leads to the generation of a bion state. From the numerical analysis we can extract the extreme values for the φ^4 system:

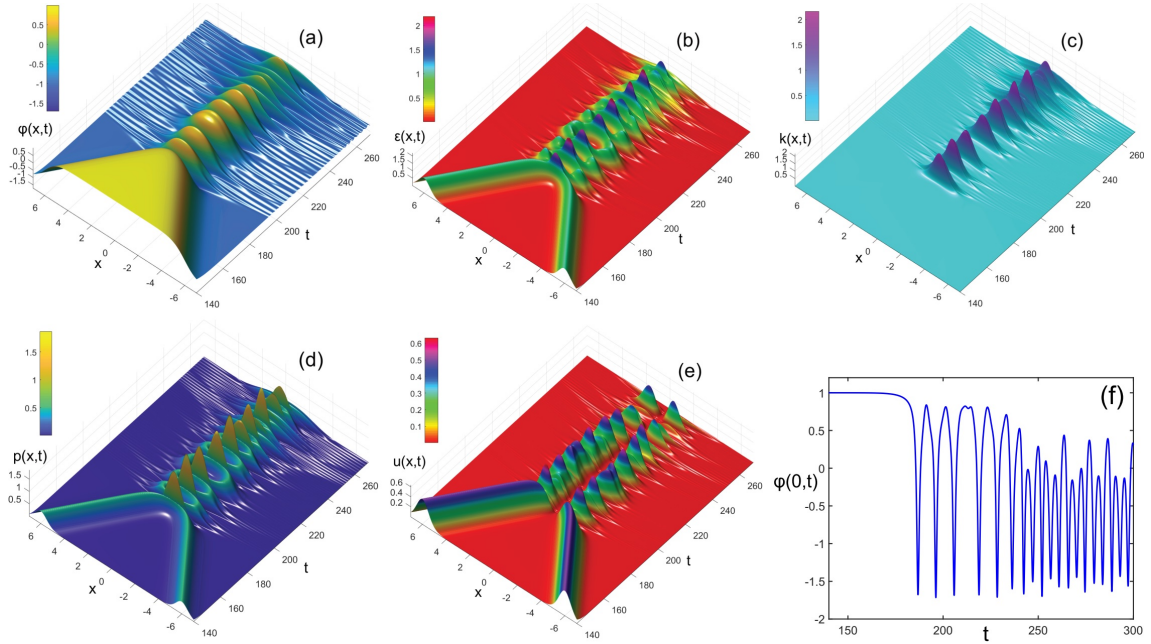


Figure 2: Some details of a kink-antikink collision in the context of φ^4 system with initial speed $v = 0.1$. Figures *a-f* represent the variation of the field, energy density, kinetic energy density, potential energy density, gradient energy density, and the field at center of mass, respectively. Note that, these explanations are similar in the following three figures and will not be repeated.

$$k_{max} = 2.1642, \quad u_{max} = 0.6332, \quad p_{max} = 1.8832, \quad \varepsilon_{max} = 2.1902. \quad (21)$$

Moreover, for the periodic φ^4 system we obtain:

$$k_{max} = 2.2452, \quad u_{max} = 0.6707, \quad p_{max} = 0.5000, \quad \varepsilon_{max} = 2.2556. \quad (22)$$

For initial speeds larger than the critical speed (i.e. $v > v_{cr}$), kink and antikink always escape from each other after collisions. As an example, some details for such collisions with $v = 0.3$ are shown in Figs. 4 and 5 for the φ^4 and periodic φ^4 systems, respectively. Furthermore, the extreme values for the φ^4 system are:

$$k_{max} = 2.0751, \quad u_{max} = 0.7530, \quad p_{max} = 1.7482, \quad \varepsilon_{max} = 2.0844. \quad (23)$$

and for period φ^4 system:

$$k_{max} = 2.0753, \quad u_{max} = 0.6623, \quad p_{max} = 0.5000, \quad \varepsilon_{max} = 2.0844. \quad (24)$$

Examining the previous four figures, one realizes that except the potential energy density p , the evolution of k , u and ε are almost similar for the two systems. Moreover,

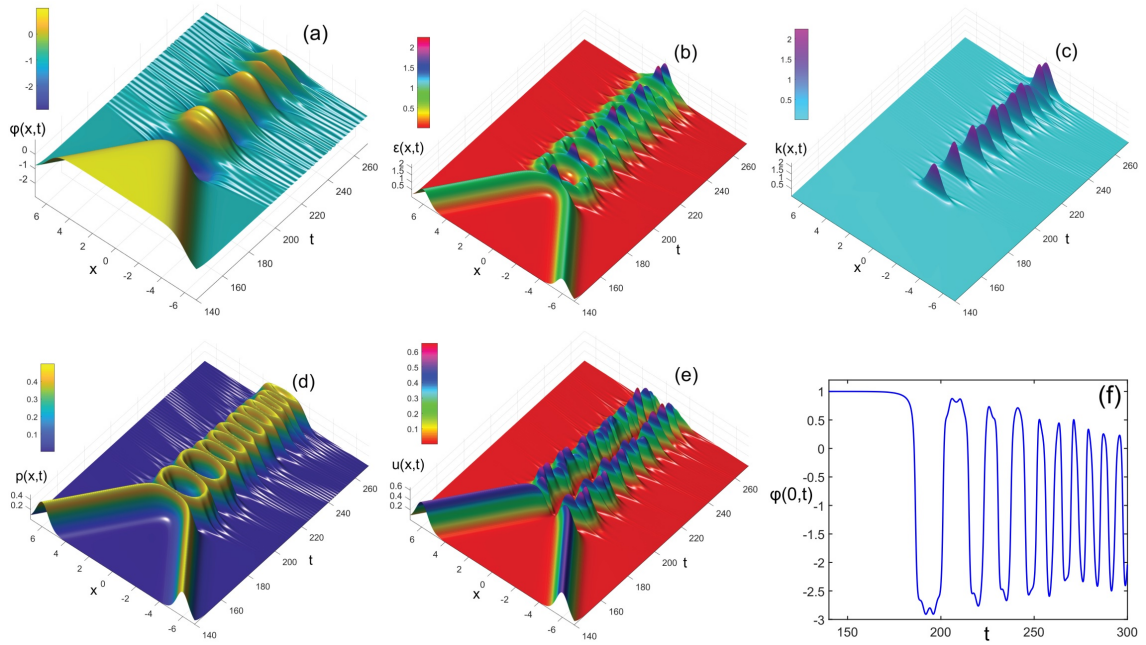


Figure 3: Some details of a kink-antikink collision in the context of periodic φ^4 system with initial speed $v = 0.1$.

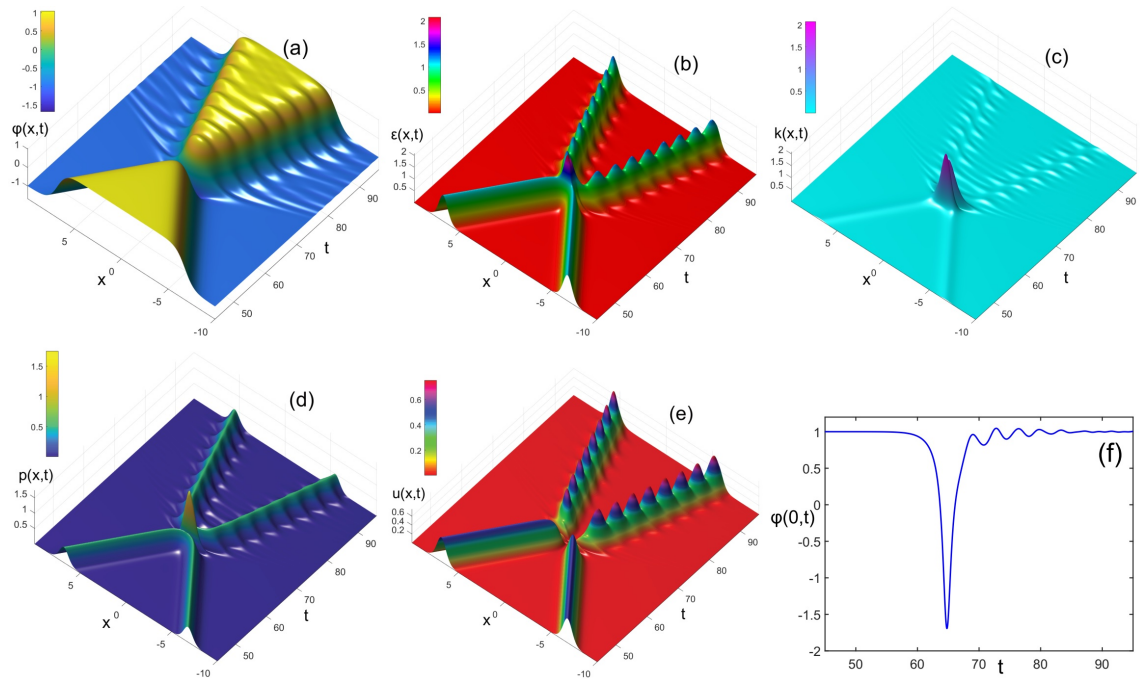


Figure 4: The details of a kink-antikink collision in the context of φ^4 system with initial speed $v = 0.3$.

comparing Eq. (21) with Eq. (22) and also comparing Eq. (23) with Eq. (24) shows that the values of p_{max} differ substantially. According to Eq. (10), p is the same potential $V(\varphi)$, and the potential of the periodic φ^4 system is confined to values less than $V(2n) = 0.5$ ($n = 0, \pm 1, \pm 2, \pm 3, \dots$), whereas the potential of the φ^4 system is not confined. In fact, for $\varphi > \sqrt{2}$, the potential of the φ^4 system is larger than 0.5. In a collision process, according to part *f* in Figs. 2-4, the field φ changes and increases (decreases) to amounts larger (smaller) than $\sqrt{2}$ ($-\sqrt{2}$). Hence, the maximum value of p in the φ^4 system would be larger than 0.5, but for the periodic φ^4 system, it would be 0.5. Furthermore, numerical analysis shows that for initial speeds larger than the critical speed of the φ^4 system, i.e.

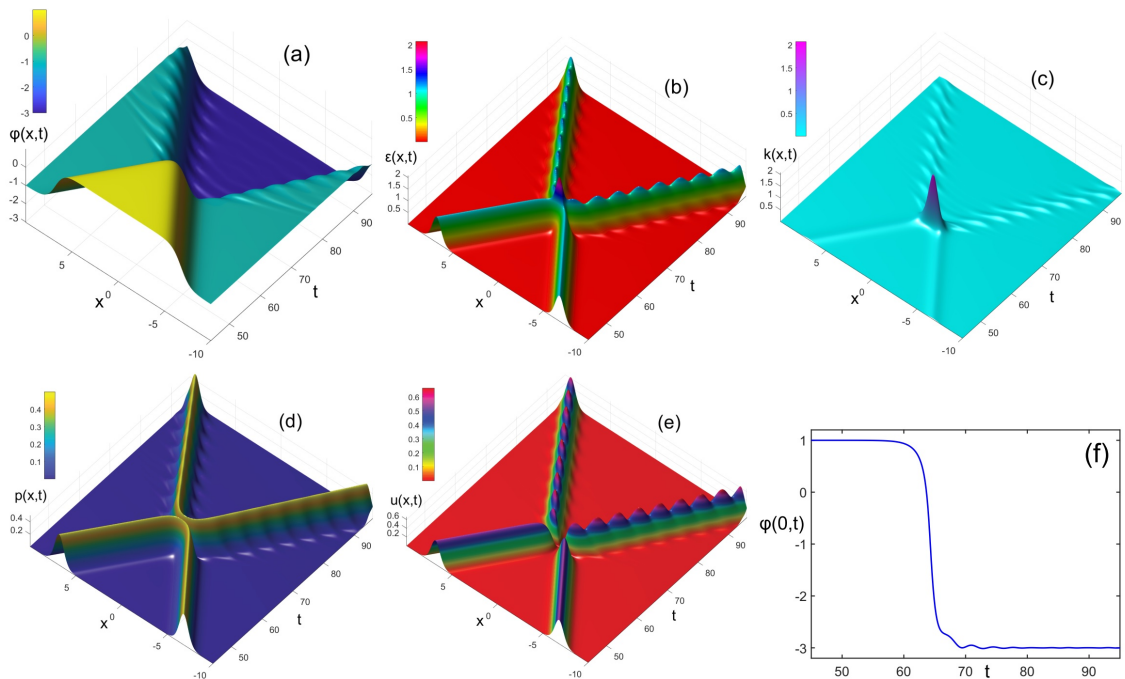


Figure 5: The details of a kink-antikink collision in the context of periodic φ^4 system with initial speed $v = 0.3$.

$v > 0.2600$, the extreme values of the energy density function are approximately the same in both systems. However, unlike the φ^4 system, for $v > v_{cr}$, a $K\bar{K}$ collision in the periodic φ^4 system, always leads to a pair of the $\bar{K}K$. Meanwhile, as Figs. 4 and 5 demonstrate, the output speed as a function of the incoming speed in the φ^4 system is always smaller than that of the periodic φ^4 system. Moreover, the amplitude of the induced vibrations after collisions, which are originated from internal modes, are smaller in the periodic φ^4 system.

4.2 The Resonance Windows

In general, for a kink-antikink collision, usually one of the three following situations will occur: Either they stick together and generate a bion state, or that they do not even feel each other's influence and get past each other having initial velocities near the speed of light. The third situation is that they bounce back and reflect from each other. For some systems, so-called radiative systems [79], there is another special situation in which the kink-antikink pair will be annihilated immediately after collision.

For many systems, including the φ^4 and periodic φ^4 system, there have been numerous wide and narrow intervals of the initial speed below v_c , instead of forming a bion, kink and antikink finally escape after finite times of collisions. For wide intervals, they usually collide for the first time, lose their kinetic energy and generate a bion state that immediately turns into a pair of kink-antikink near the collision point. They collide for the second time generating another bion state which leads to a pair of kink-antikink that gets separated and travel back to their starting points. This phenomenon is known as the two-bounce resonance [31, 75, 82]. Thus, the interesting part is finding intervals of the initial speeds which lead to two-bounce resonances, such a special interval is called a two-bounce (scattering) window. In Fig. 6, for instance, a two-bounce resonance is shown for systems φ^4 and periodic φ^4 , respectively.

For better understanding, for many kink-antikink collisions, we prepared the output speed as a function of the incoming speed for the φ^4 (periodic φ^4) system in the range from 0.18 to 0.28 (0.1 to 0.16) with the small step size 0.00001, numerically. The final result of the time-consuming computation is Fig. 7-a (b) for the φ^4 (periodic φ^4) system.

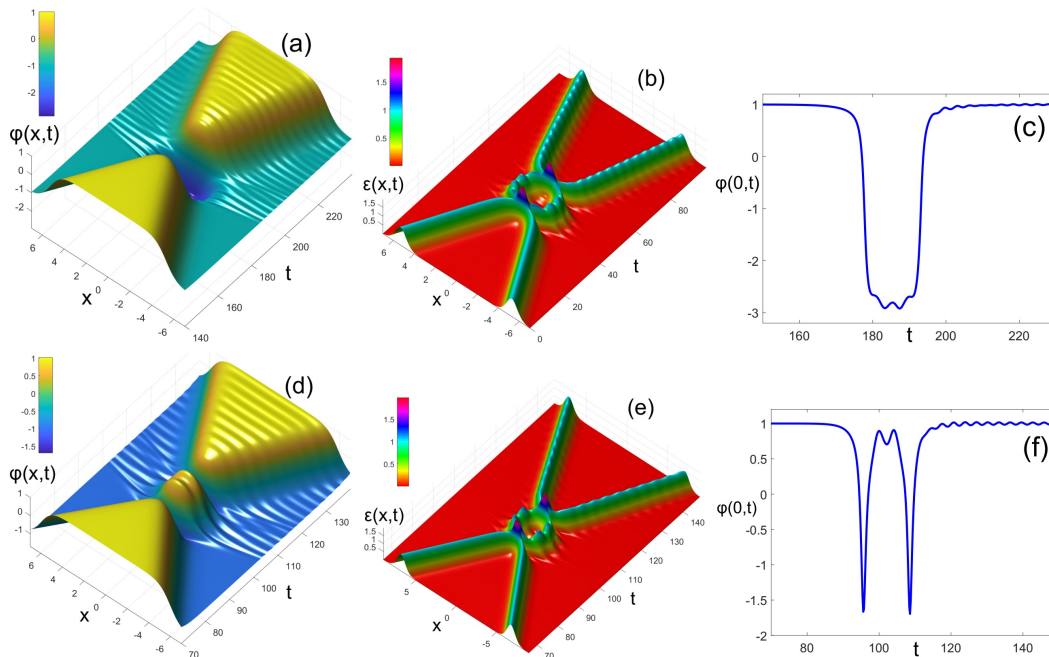


Figure 6: The second (first) row shows a two-bounce resonance in the context of the φ^4 (periodic φ^4) system with the initial speed $v = 0.2$ ($v = 0.105$). Figures *a* and *d* show the field representations, Figs. *b* and *e* show the energy density representation, and Figs. *c* and *f* show the variation of the fields at the center of mass $\varphi(0, t)$ for these collisions.

We split the obtained peaks into two groups of blue (purple) and red. The intervals where the blue (purple) peaks are located represent the two-bounce windows of the φ^4 (periodic φ^4) system. Different blue (purple) peaks corresponding to different two-bounce scattering windows are counted from left to right depending on their position on the v_{in} -axis. Red peaks are usually another type of windows known as three-bounce windows that will be discussed subsequently. In general, it seems that there are many discrete two-bounce windows that the width of them decreases as the initial speeds increase. Numerical calculation shows that the $(n + 1)$ th two-bounce window differ from (n) th two-bounce window by a longer time interval, corresponding to an additional cycle oscillation between their first and second collisions [31] (see Fig. 8 and Fig. 9). In this regard, a peak to peak time interval (T_{pp}) can be introduced for the small cycle oscillations to be used as a criterion for comparing the time elapsed between the first and second collisions in different two-bounce scattering windows (see Fig. 8). Figure 9 illustrates the relation between the peak to peak time interval (T_{pp}) and the number of different two-bounce windows (n). For both φ^4 and periodic φ^4 systems, this relation is linear with a very good approximation. Moreover, Fig. 9 shows that the green and red dots coincide very well together, indicating that the two systems behave similarly for these small oscillations. Furthermore, it should be noted that only for the periodic φ^4 system, there are seen another type of very narrow detached intervals for which two bion states reappear after kink-antikink collisions (see Fig. 10), that is, the intervals correspond to the green peaks in Fig. 7-*b*.

Around the wide blue (purple) peaks in Fig. 7, there are many narrow red peaks, which indicate another type of scattering windows known as three-bounce scattering windows, in which kink and antikink collide three times and then recede (see Fig. 11). In general, there is a quasi-fractal structure for such peaks (corresponding to scattering windows), that is, for any narrow n -bounce window, corresponding to a sharp peak, there are some adjacent sharper peaks which indicate a group of narrower $(n + 1)$ -bounce windows. An n -bounce window is an interval of initial speed for which kink and antikink collide n times before bouncing back. For example, zooming in on the first two-bounce window of the φ^4 system in Fig. 7-*a* in the range of 0.18 to 0.21, leads to Fig. 12-*a*. Among the sharp peaks around

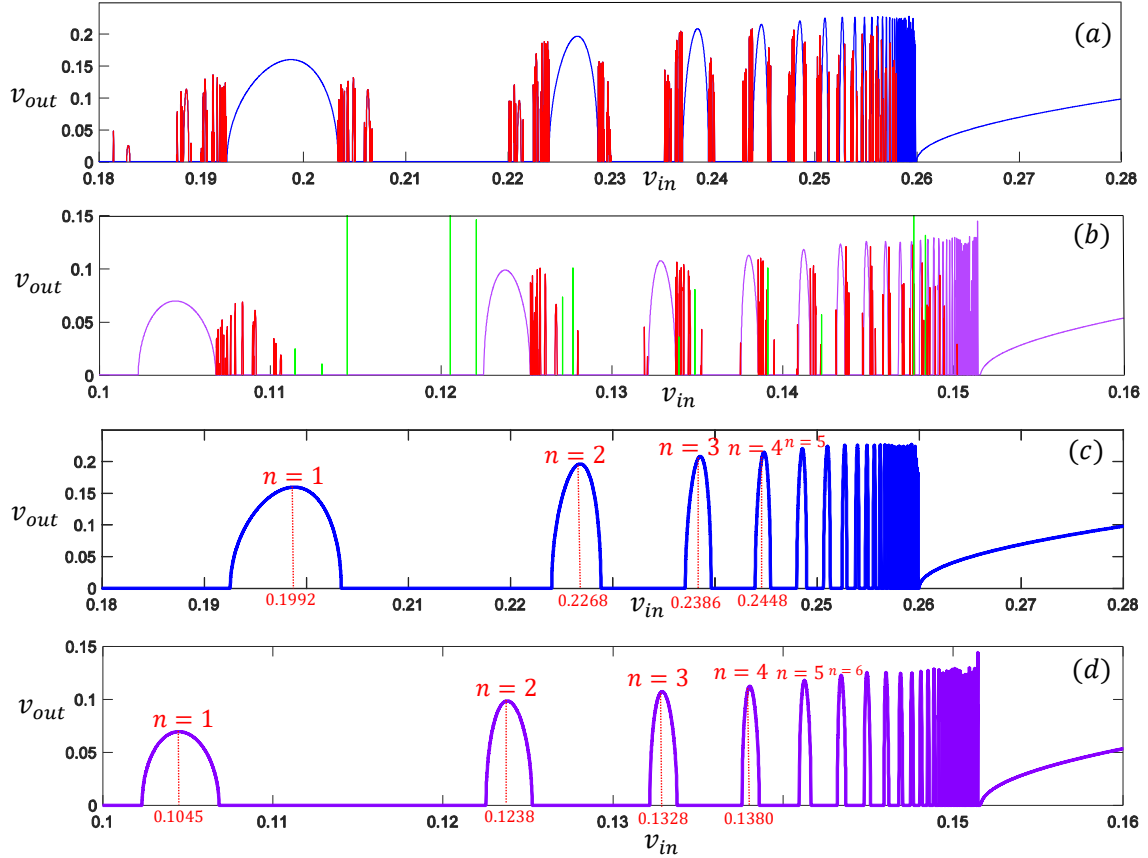


Figure 7: The output velocity versus the input velocity. Figures *a* and *c* (*b* and *d*) belong to φ^4 (periodic φ^4) system. Blue and purple peaks are the two-bounce resonance windows and they can be labeled by incremental integers from left to right. The other red sharp peaks are usually the three-bounce resonance windows which accumulated almost symmetrically (asymmetrically) around the two-bounce resonance windows of the φ^4 (periodic φ^4) system. The very sharp green peaks in Fig. *b* demonstrate the situations for which the kink-antikink collision eventually leads to a pair of bion states.

the first two-bounce window, we can consider a small interval containing a sharp peak, i.e. the red part in Fig. 12-*a* (for simplicity we refer to it as the red interval). If we divide the red narrow interval into 1000 nodes, and perform the numerical calculation for all of them, a more accurate $v_{out} - v_{in}$ diagram for this interval can be obtained (see Fig. 12-*b*), which shows some new detail for the red small interval. Note that, since Fig. 12-*a* is obtained by dividing the interval 0.18 to 0.21 into 300 nodes, the red interval is then approximated to only 7 nodes, which is not enough to acquire sharper peaks around the red peak in Fig. 12-*a* numerically.

Again, we can choose another small interval containing a sharp peak in Fig. 12-*b*, i.e. the blue region, and then a more accurate diagram with 1000 nodes can be obtained (see Fig. 12-*c*). This routine was repeated for the small green and purple intervals in next figures. Hence, the more we repeat the zooming in process, the sharper peaks will be revealed. What we can see here is the existence of a quasi-fractal structure which can be considered as a general rule for any small interval containing a peak (in fact a n -bounce window), that is, we can see that there are other sharper peaks to the left and right each original peak. Similar results are noticed for all peaks in the $v_{out} - v_{in}$ diagram of the periodic φ^4 system, as well (see Fig. 13). However, the more interesting rule is that if a special peak corresponds to an n -bounce window, the surrounding left and right peaks are usually $(n + 1)$ -bounce windows. To give an example, the wide smooth purple peak in Fig. 13-*e* is corresponding to a 6-bounce scattering window and the three sharp peaks

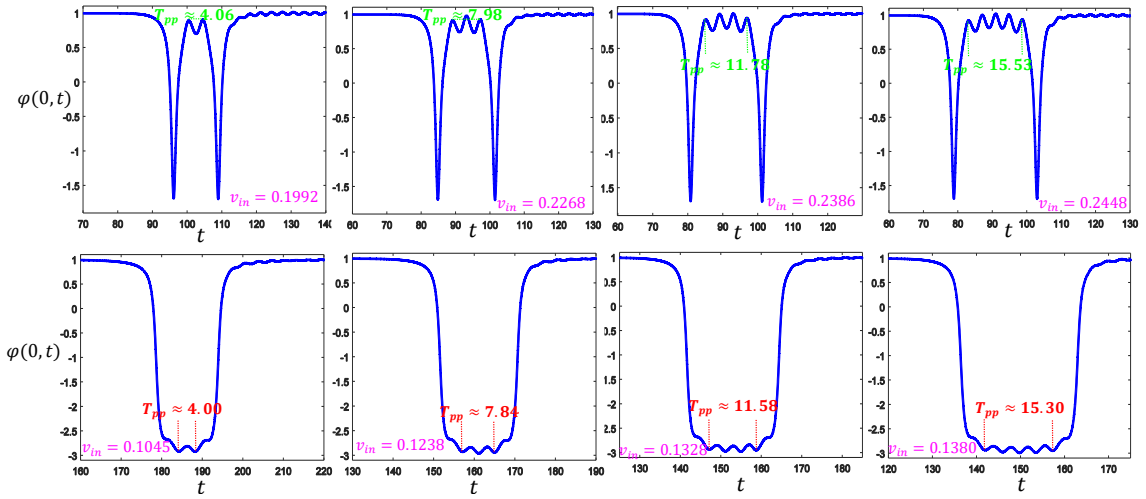


Figure 8: The variation of the field at the center of mass of a kink-antikink collision for different initial velocities belong to first, second, third, and fourth two-bounce windows. First (second) row belongs to the φ^4 (periodic φ^4) system. The $(n + 1)$ th two-bounce window differs from (n) th two-bounce window by a longer time interval between its first and second collision, and an additional cycle oscillation. The peak to peak time intervals are introduced in these figures.

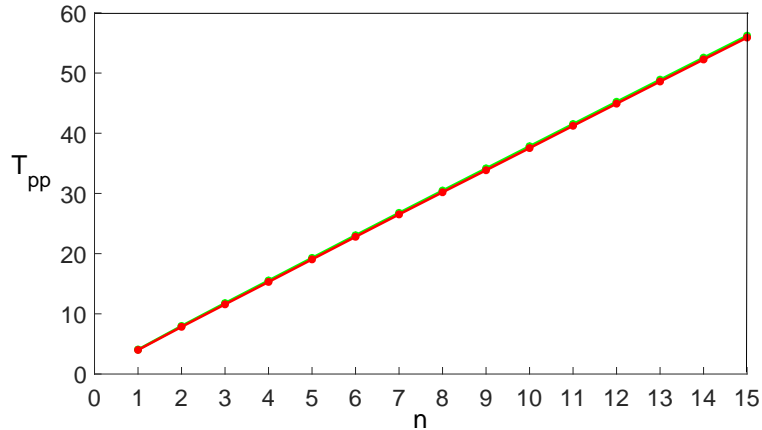


Figure 9: The peak to peak time intervals T_{pp} (see Fig. 8) versus the order of different two-bounce scattering windows (see label n in Fig. 7). The green (red) dots show the results of our numerical calculations for the φ^4 (periodic φ^4) system. Although the two systems have different potentials for regions $\varphi < -1$, and $\varphi > 1$ and different $v_{out} - v_{in}$ diagrams, interestingly they exhibit almost similar behavior in relation to the time elapsed between successive collisions.

around it are actually 7-bounce scattering windows. The reported phenomena in the φ^4 and in the periodic φ^4 systems were studied before not only in the φ^4 system [31,75,82], but also in the modified sine-Gordon equation [74] and in the double sine-Gordon model [32].

It should be noted that in the figures obtained (12 and 13), the more we zoom in, the narrower intervals are obtained with more decimal numbers. Hence, the numerical results for such very narrow intervals, due to the high sensitivity and inevitability of numerical errors, would depend on the type of space-time spacing. Figures *d* and *e* were obtained for $h = k = 0.02$ and may be changed if we use other space-time spacing values. However, the original nature of these systems does not change and is similar to what was seen in Figs. 12 and 13 by zooming in.

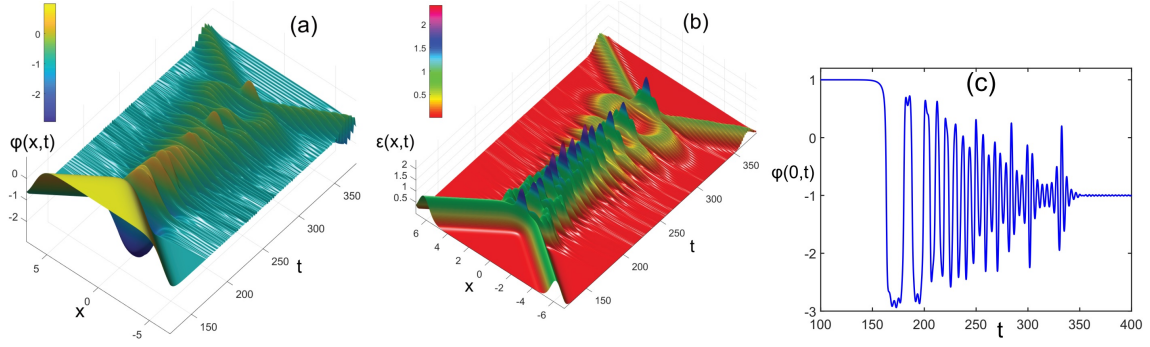


Figure 10: Generation of a pair of bion states in a kink-antikink collision of the periodic φ^4 system with the initial speed $v = 0.11454$. This is not the case for the φ^4 system.

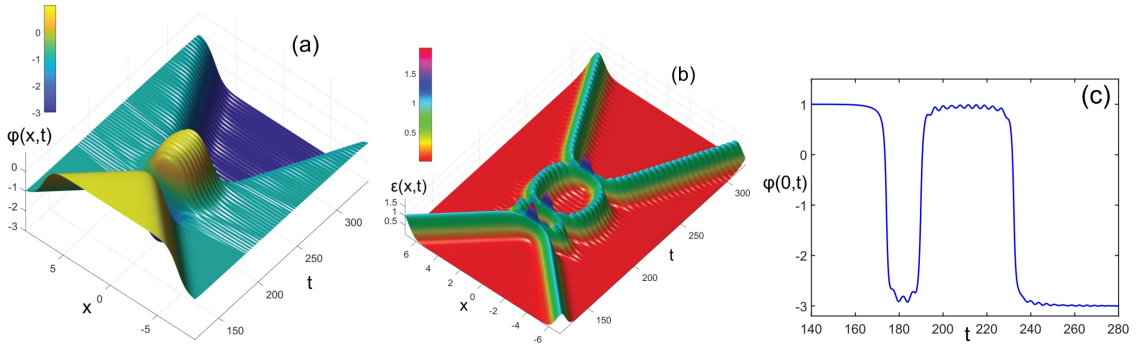


Figure 11: Three-bounce resonance in a kink-antikink collision of the periodic φ^4 system with the initial speed $v = 0.10722$.

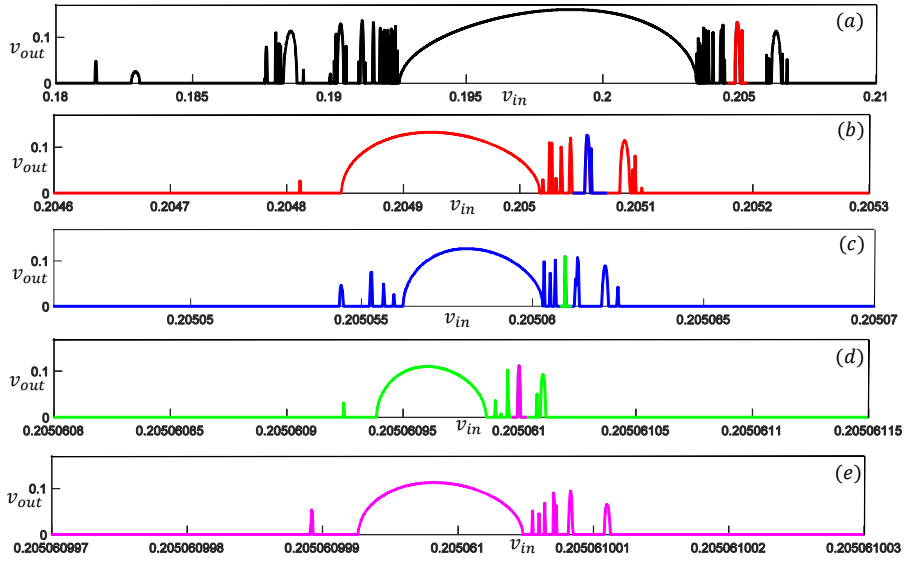


Figure 12: The quasi-fractal structure for the φ^4 system in $v_{out}-v_{in}$ diagram.

4.3 Disturbed kink-antikink Collisions

To study a disturbed kink-antikink collision with the initial velocities v and $-v$ and initial positions a and b (provided $|b - a|$ is large enough), for which at least one of the kink and antikink solutions get excited, we first need to prepare the initial conditions in the following form:

$$\phi_{K\bar{K}}(x, t) = \tanh(+\gamma(x - vt - a)) + \psi_1(\gamma(x - vt - a)) \sin(\omega t - kx + \theta_1) + \tanh(-\gamma(x + vt - b)) + \psi_2(\gamma(x + vt - b)) \sin(\omega t + kx + \theta_2) - 1, \quad (25)$$

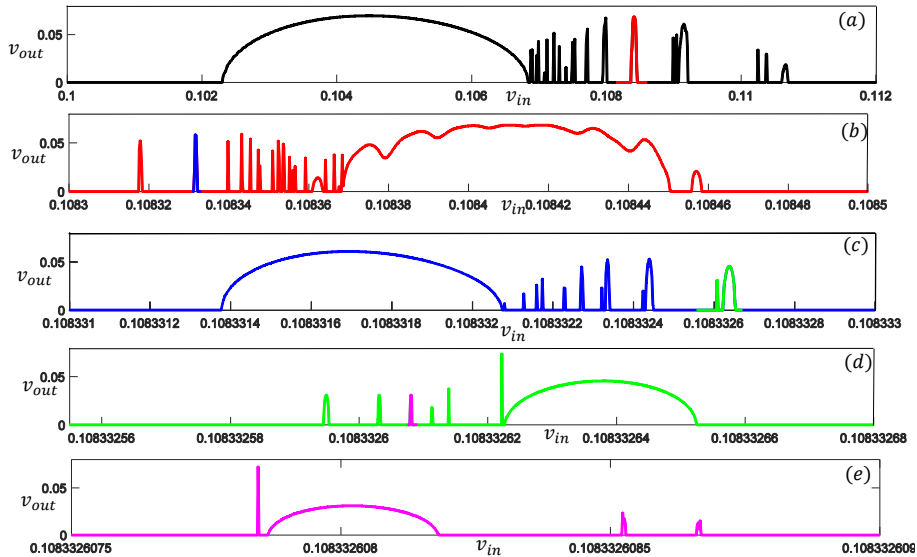


Figure 13: The quasi-fractal structure for the periodic φ^4 system in v_{out} - v_{in} diagram.

where $\psi_1(x)$ and $\psi_2(x)$ are linearly dependent small functions, θ_1 and θ_2 are two arbitrary initial phases of the kink and the antikink, respectively. Although $\psi_1(x)$ and $\psi_2(x)$ are small and do not change the particle features of the distinct kink and antikink at initial times significantly, it can be shown numerically that the small trapped wave profiles by kink and antikink, i.e. $\psi_1(\gamma(x-vt-a)) \sin(\omega t - kx + \theta_1)$ and $\psi_2(\gamma(x+vt-b)) \sin(\omega t + kx + \theta_2)$, have a crucial role in the output of the collisions. In fact the maximum amplitudes of trapped wave-profiles $A_1 = \max \psi_1$ and $A_2 = \max \psi_2$, and initial phases θ_1 and θ_2 , are two important factors that can have a significant impact on the outcome of the collisions. Note that, the initial phases θ_1 and θ_2 are completely optional parameters which can be randomly considered any amount in the initial conditions (25), however, they play an important role in the fate of a disturbed kink-antikink collision.

For example, for φ^4 and periodic φ^4 systems, the red (blue) curves in Fig. 14 show how the output speed of a kink in a disturbed kink-antikink collision with $b = -a = 20$, $v = 0.2$, $A_1 = A_2 = 0.1$ ($= 0.05$), and $\theta_1 = 0$, is affected by different optional choices of the initial phase θ_2 . Moreover, we obtain the output velocity of the disturbed kink-antikink collisions versus the maximum amplitudes of the initial wave profiles $A_1 = A_2 = A$ in Fig. 15 for the φ^4 and periodic φ^4 systems, we set $\theta_1 = \theta_2 = 0$, $b = -a = 20$, $v = 0.2$. Numerically, it was seen that high speed collisions (energetic collisions) reduce the influence of the initial trapped wave profiles on the fate of collisions, i.e. we do not see significant different outcomes in the outputs.

In Figs. 14 and 15, there are intervals for which a chaotic behavior is seen. Similar to quasi-fractal structure of resonance windows which was discussed in the pervious subsection, here it was seen that the peaks in these special intervals have a quasi-fractal structure as well. For instance, we can consider a small interval containing a sharp peak in the chaotic region of the red curve in the Fig. 15-b, i.e. the blue part in the Fig. 16-a. According to Fig. 16, if we repeat the numerical simulation by 500 nodes just for the blue narrow interval, a more accurate Fig. (16-b) is obtained which shows some new detail for the blue interval. Again, we can choose another narrower interval containing a sharp peak in Fig. 16-b, i.e. the green part, and using a more accurate simulation with more nodes to lead to Fig. 16-c, and so on for the pink and orange small intervals in the next figures.

What we can observe here is the existence of a quasi-fractal structure which can be considered to be a general rule for any small interval containing a peak in any chaotic area. That is, as a rule, other sharper peaks surround each original peak from left and right. In the pervious subsection, to show that there is a quasi-fractal structure, we studied the outgoing velocity versus the incoming velocity to obtain the intervals with sharp peaks.

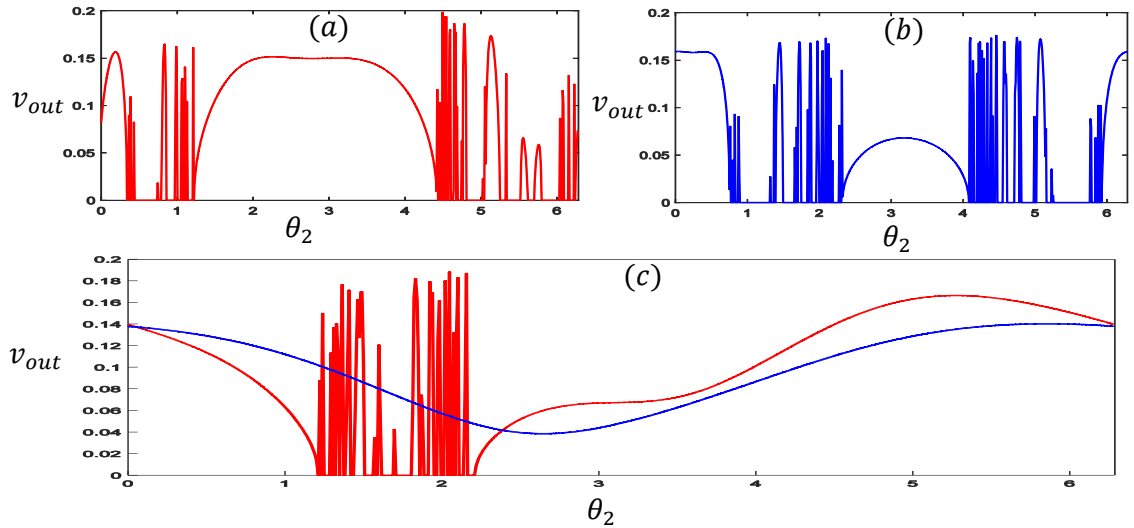


Figure 14: The output velocity versus θ_2 for a disturbed kink-antikink collision. Figs-*a* and *b* are obtained in the context of the φ^4 system and Fig-*c* is obtained in the context of the periodic φ^4 system. For the red (blue) curves the maximum amplitude of the initial trapped wave profile is $A = 0.1$ ($A = 0.05$). Disturbed kink and antikink initially stand at $a = -20$ and $b = 20$, the initial speed is $v = 0.2$, and for disturbed kink $\theta_1 = 0$. To obtain these results, we used 700 nodes for θ_2 in the range from 0 to 2π .

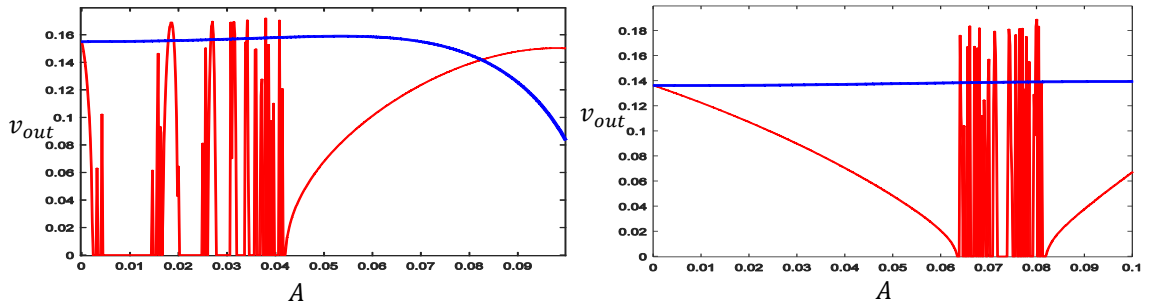


Figure 15: The left (right) figure presents the output velocity versus $A = A_1 = A_2$ for a disturbed kink-antikink collision with $v_{in} = 0.2$ in the context of the φ^4 (periodic φ^4) system. For the blue (red) curve the initial phases are $\theta_1 = \theta_2 = 0$ ($\theta_1 = 0$ and $\theta_2 = \pi$). To obtain this figure we study all collisions in the range $0 < A < 0.1$ with 500 nodes.

Moreover, it was found that if any peak is an n -bounce window, the surrounding sharper peaks are usually $(n + 1)$ -bounce windows. A similar result is also obtained here for intervals with sharp peaks in the v_{out} - A diagrams. In fact, for any sharp peak in the v_{out} - A diagram, we can define another type of windows with respect to parameter A which can be called an A -window. Studying the peaks in Fig 16 *a-e*, shows that if a special peak corresponds to an n -bounce A -window, a substantial number of peaks surrounding it, are $(n + 1)$ -bounce A -windows (see Fig. 17). Therefore, there is a similar quasi-fractal structure in chaotic regions of v_{out} - A diagrams as well as the $v_{out} - v_{in}$ diagram. These results can be generalized to the $v_{out} - \theta$ diagrams as well. To clarify, according to Fig. 14-*b*, we can select a special peak among the others in Fig. 18-*a* with the red color. Similar to the same process described in detail earlier, we show the results in Figs. 18 and 19 for $v_{out} - \theta_2$ diagrams. For a more accurate analogy, it may be better to call the discussed windows in the $v_{out} - v_{in}$ diagrams, v_{in} -windows.

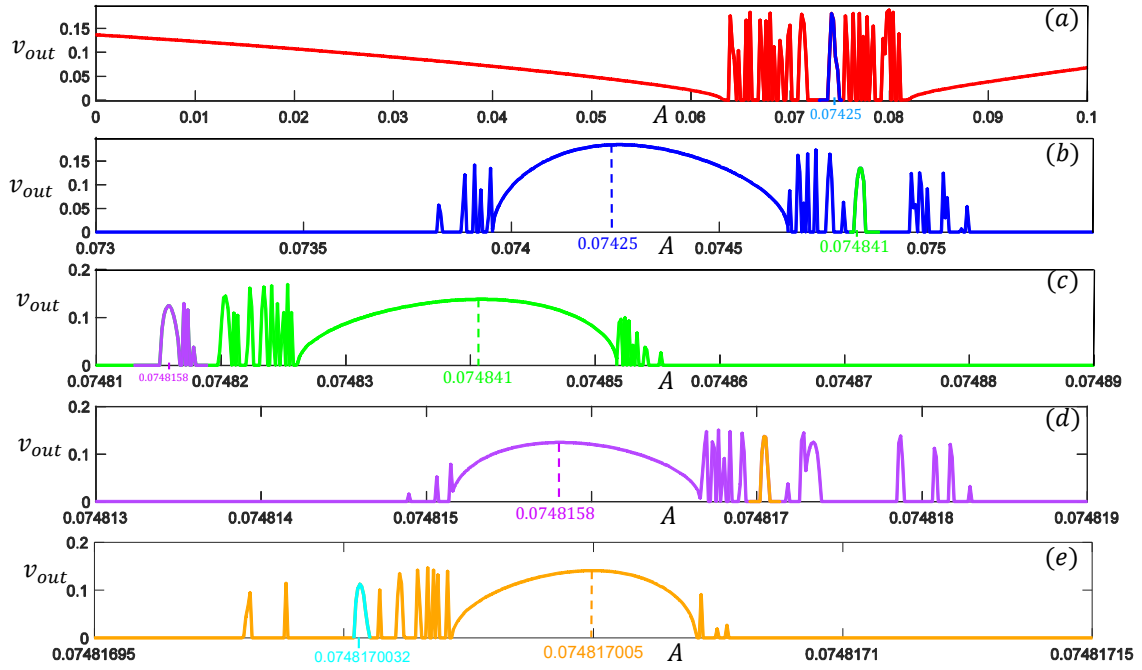


Figure 16: The quasi-fractal structure for the periodic φ^4 system in v_{out} - A diagram. The blue peak in Fig-a, the green peak in Fig-b, the smooth part of the purple peak in Fig-c, the orange peak in Fig-d, and the cyan peak in Fig-e are related to a two-bounce, three-bounce, four-bounce, five-bounce, and a six bounce A-window, respectively. A similar explanation can be used for v_{in} -windows in Figs. 12 and 13.

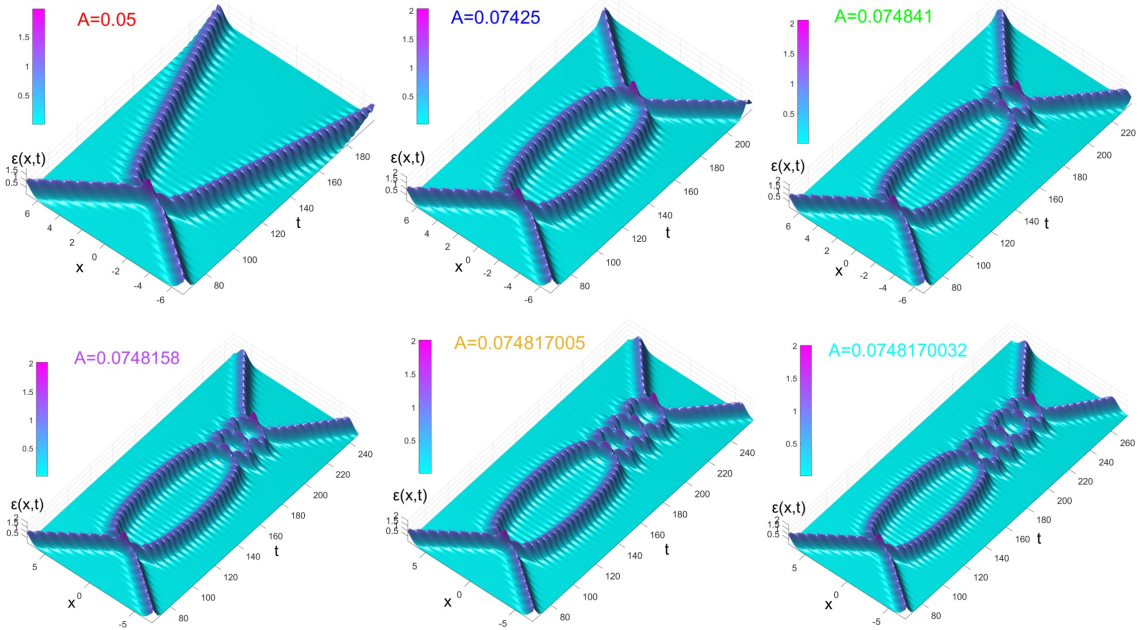


Figure 17: The energy density representation of six disturbed kink-antikink collisions with different values of A in the context of the periodic φ^4 system. We set $v = 0.2$, $\theta_1 = 0$, and $\theta_2 = \pi$. For different peaks (A -windows) in Fig. 16, different n -bounce ($n = 2, 3, 4, 5, 6$) collisions would occur.

4.4 The Collision of kink-antikink-kink

In this case we study the results of the collisions between two kinks and one antikink ($K\bar{K}K$). We set the initial conditions so that all the participants arrive at one point (origin) simultaneously. The kinks, which are placed at $x_3 = -x_1 = 20$, are moving

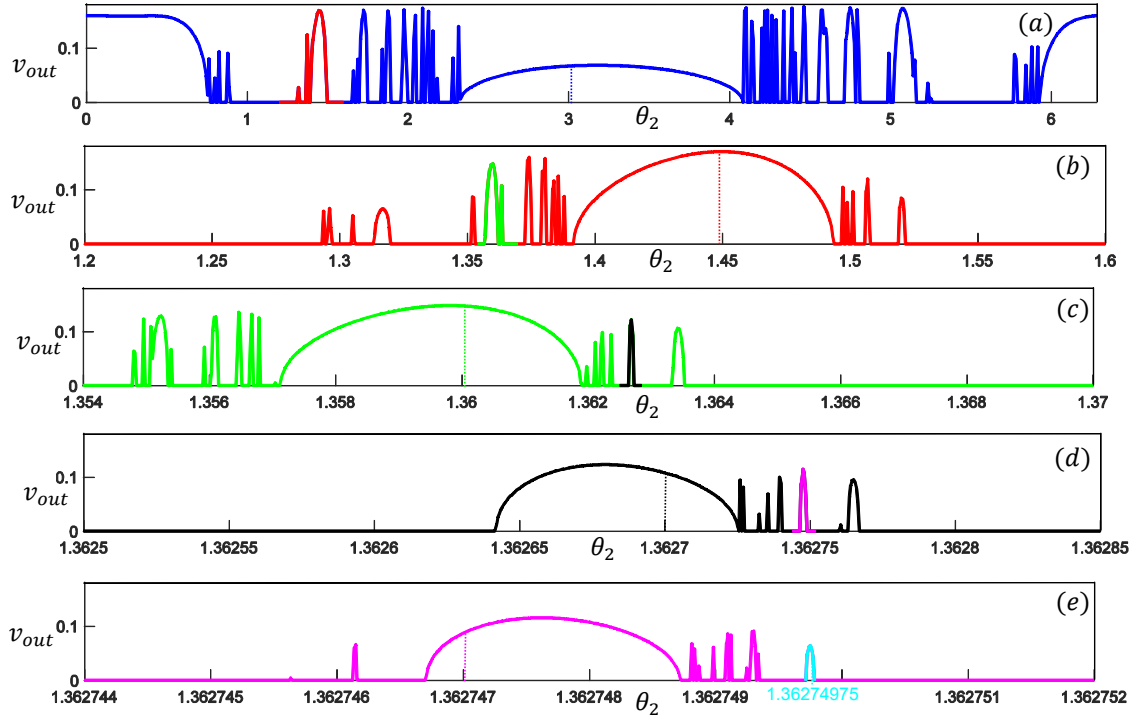


Figure 18: The quasi-fractal structure for the φ^4 system in $v_{out}-\theta_2$ diagram. The blue peak in Fig-a, the green peak in Fig-b, the black peak in Fig-c, the purple peak in Fig-d, and the cyan peak in Fig-e are related to a two-bounce, three-bounce, four-bounce, five-bounce and a six-bounce θ_2 -window, respectively.

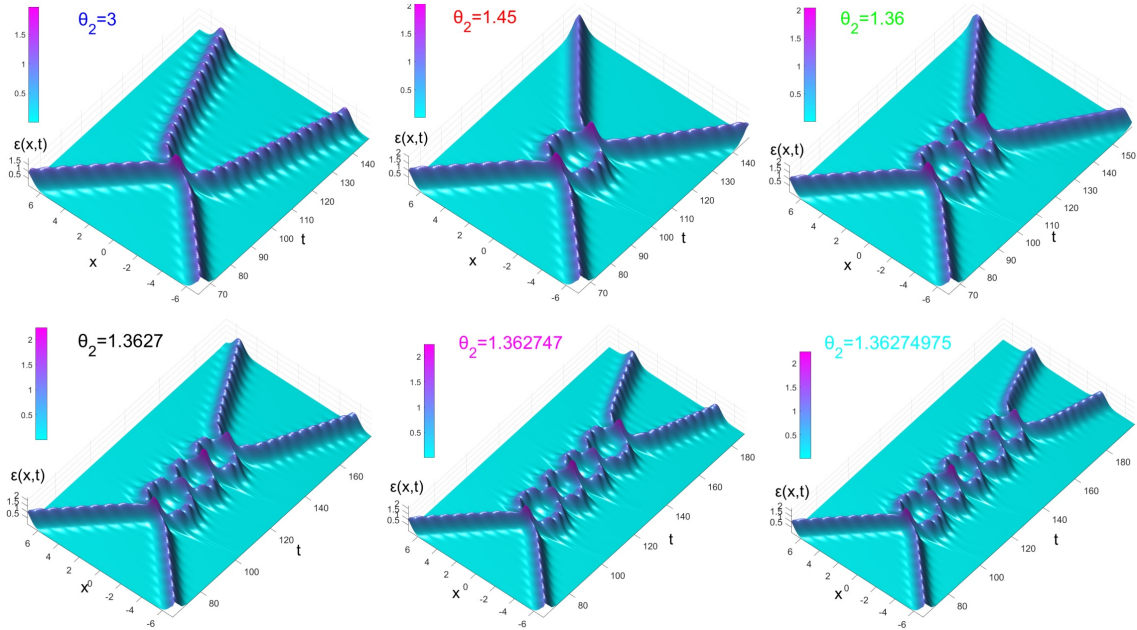


Figure 19: The energy density representation of six disturbed kink-antikink collisions with different values of θ_2 in the context of the φ^4 system. We set $v = 0.2$, $\theta_1 = 0$, and $A = 0.05$. For different peaks (θ -windows) in Fig. 18, different n -bounce ($n = 2, 3, 4, 5, 6$) collisions would occur.

towards the antikink placed at the origin ($x_2 = 0$) with the same speed. The proper initial condition for this situation is:

$$\varphi_{K\bar{K}K} = \tanh(+\gamma(x - vt - x_1)) + \tanh(-(x - x_2)) + \tanh(\gamma(x + vt - x_3)). \quad (26)$$

In the context of the φ^4 system, the critical speed is about $v_{cr} = 0.7650$ for which if $v < v_{cr}$, eventually a single at rest vibrating antikink remains (Fig. 20-a), and if $v \geq v_{cr}$, the orientation $K\bar{K}K$ will reappear after the collision (Fig. 20-b). Only for the four narrow intervals of incoming speeds (yellow bars in Fig 21-b), close to the critical speed, $K\bar{K}K$ reappear after the collisions. In fact, we can extend the concept of scattering windows for the $K\bar{K}K$ collisions, that is, there are some special intervals of initial incoming velocities slower than the critical speed for which $K\bar{K}K$ can scatter each other, but they are always two-bounce scattering windows. At the edge of the scattering windows, another interesting phenomenon was observed which is the appearance of a vibrating antikink plus a bion state that both leave the collision area in the opposite directions (Fig. 20-c).

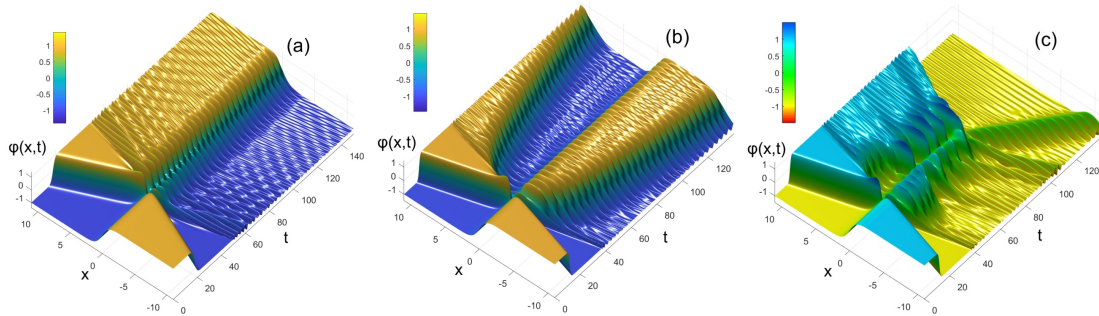


Figure 20: The field representations of the $K\bar{K}K$ collisions in the context of the φ^4 system. For plots-a, b, and c, the initial speed is $v = 0.5$, $v = 0.765$, and $v = 0.7591$, respectively.

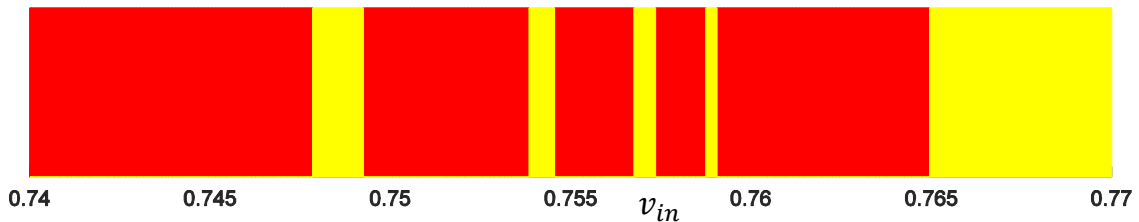


Figure 21: Different fates versus incoming speed for the $K\bar{K}K$ collisions in the context of the φ^4 system. The red and yellow bars correspond to the intervals which leads to a single vibrating kink and the reappearance of the triad $K\bar{K}K$, respectively. In fact, four narrow yellow bars indicate four scattering windows. To obtain this figure we studied all collisions in the range $0.74 < v_{in} < 0.77$ with the step size of 0.0001.

For periodic φ^4 system, studying the $K\bar{K}K$ collisions leads to different scenarios. Again, if the initial speed is higher than a critical speed of about $v_{cr} = 0.3335$, the orientation $K\bar{K}K$ will reappear after the collisions (see Fig. 22-c). Although, for the initial speeds smaller than v_{cr} , there are different intervals for the incoming speeds with different outcomes. More precisely, for $K\bar{K}K$ collisions with $v < 0.3335$, there are four different scenarios at the end (see Fig. 23). First, a vibrating antikink and a bion state remain and leave the collision area in the opposite directions (see Fig. 22-a and the blue bars in Fig. 23). Second, similar to Fig. 20-a, only a standing vibrating antikink remains (see the red bars in Fig. 23). Third, a vibrating antikink and two moving bion states remain (see Fig. 22-b and the green bars in Fig. 23). Fourth, the triad $K\bar{K}K$ reappear after collisions (see Fig. 22-c and the yellow bars in Fig. 23). The fourth case particularly characterizes the (two-bounce) scattering windows for the $K\bar{K}K$ collision in the context of the periodic φ^4 system.

Accordingly, the study of three soliton-like collisions clearly shows us that despite the similarity of the potential in the range from -1 and 1 for both systems (and then the similarity of the kink and antikink), the output of the collisions depends strongly on the potential in other ranges. In sum, the periodic φ^4 system provides a richer structure and

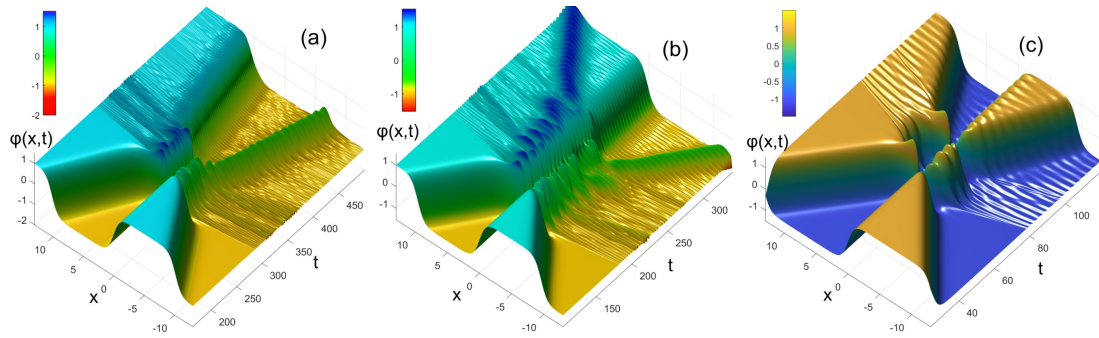


Figure 22: The field representations of $K\bar{K}K$ collisions in the context of the periodic φ^4 system. For plots-*a*, *b*, and *c*, the initial speed is $v = 0.06$, $v = 0.1$, and $v = 0.28$, respectively.

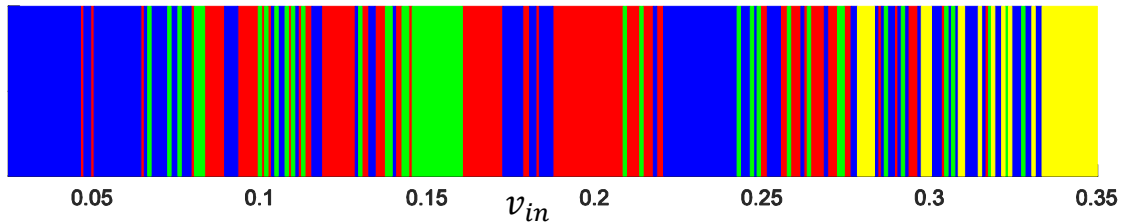


Figure 23: Variety of different fates versus incoming speed of the $K\bar{K}K$ collisions in the context of the periodic φ^4 system. The blue, red, green, and yellow bars are showing different intervals of incoming velocities which in turn lead to a bion state plus a vibrating kink, a single vibrating kink, two bion states plus a vibrating kink, and the reappearance of the triad $K\bar{K}K$. To obtain this figure we studied all collisions in the range $0.025 < v_{in} < 0.350$ with the step size of 0.001.

more detail to study.

5 Summary and Conclusion

Based on the potential of the well-known relativistic kink-bearing φ^4 system, we introduced a new system that we call the periodic φ^4 system. The potential function in both systems is the same in the range $-1 \leq \varphi \leq 1$ which is corresponding to a kink (antikink) solution. But for the periodic φ^4 system, we use the same potential periodically in the range $-1 \leq \varphi \leq 1$ for other ranges from ± 1 to $\pm\infty$. As long as we are dealing with a single kink (antikink), everything is the same, and there is no difference between the two systems in terms of physical properties, but when it comes to interaction with an antikink (a kink), due to the potential difference in the other ranges, behaviors are practically different. This paper attempts to provide a comparative study of the properties of two systems in interactions.

We have implemented a numerical program with proper accuracy in MATLAB, based on a fourth-order Runge-Kutta scheme to simulate the collisions (interactions). We studied the kink-antikink collisions to obtain the scattering windows and other properties of both systems. For the φ^4 (periodic φ^4) system, the critical speed is about $v_{cr} = 0.2600$ ($v_{cr} = 0.1516$). Usually for the speeds less than the critical speed, kink and antikink stick together and produce a bion state. However, in this range of initial speeds, there are many wide and narrow intervals that the pair of kink-antikink can scatter from one another. Such intervals on the axis of the incoming speed (v_{in}) are called the scattering windows (in this paper we call them v_{in} -windows). The wide intervals in this range are two-bounce v_{in} -windows, and the surrounding narrow intervals are 3-bounce v_{in} -windows. For the two-bounce v_{in} -windows, it was seen numerically that the time interval between the first and

second collisions increases in a linear fashion versus the number of successive two-bounce v_{in} -windows approximately in the same way for both systems. Around the three-bounce v_{in} -windows, there are some narrower intervals which are 4-bounce v_{in} -windows, and so on, that is, there exists quasi-fractal structures for both φ^4 and periodic φ^4 systems in $v_{out} - v_{in}$ diagram where $v_{in} < v_{cr}$. The notable difference in $v_{out} - v_{in}$ diagrams is that the peaks around the two-bounce v_{in} -windows in the φ^4 system are symmetrically distributed to the left and right, but for the periodic φ^4 system, they mainly appear to the right of them. Furthermore, another interesting phenomenon in studying the kink-antikink collisions of the periodic φ^4 system (that is not the case of the φ^4 system) is the existence of very narrow intervals of the initial speeds for which a pair of bion states appear as a result of a kink-antikink collision. This phenomena were also observed in [42, 47, 63], that called a *bound state of two oscillations*".

Since the kink and antikink in φ^4 (periodic φ^4) system have a non-trivial internal mode, they can get excited and have a constantly internal vibrational motion after each collision. This internal motion can be specified by two parameters: amplitude of the trapped wave profile A and the initial phase θ . For the same initial speeds larger than the critical speeds, the amplitude of the imposed internal vibrations on the kink and antikink after the collisions, in the context of the periodic φ^4 system, are smaller than that of the φ^4 system, thus, the output speeds are higher in value in the periodic φ^4 system. In a disturbed kink-antikink collision, for which at least one of the kink and antikink get excited, the study of $v_{out}-A$ and $v_{out}-\theta$ diagrams at a constant incoming speed show that we can introduce other types of scattering windows on the axis of A and θ , which can be called A -windows, and θ -windows. For such windows, we noticed a quasi-fractal structure similar to v_{in} -windows.

By looking at Figs. 12 (a-e), 13 (a-e), 16 (b-e), and 18 (b-e), it seems there is a general rule for the fractal structure in φ^4 and periodic φ^4 systems. In fact, in the context of the φ^4 (periodic φ^4) system, for any wide peak, if the selected sharp peak (which is identified by a different color) is on the right of that, in the next step, the surrounding sharper peaks are mainly on the right (left). The same statement can be reused by replacing the words left and right. For example, in Fig. 16-c which was obtained for the φ^4 (periodic φ^4) system, we select a sharp purple peak on the left of the wide green peak, then in the next Fig. 16-d, the main surrounding sharper peaks are on the right. As another example, in Fig. 18-d, the selected sharp purple peak on the right side of the wide black peak, leads to a wide purple peak with some surrounding sharper peaks mainly located on the right side of that.

Considering the collisions of three solitons ($K\bar{K}K$) in both systems and comparing them, show that the diversity of phenomena in the periodic φ^4 is richer than the φ^4 system. For both systems, there are different critical speeds, that $K\bar{K}K$ always scatter from each other and reappear after the collisions with $v > v_{cr}$. In the context of the periodic φ^4 system, the collision of the $K\bar{K}K$ for $v < v_{cr}$ occur in four different scenarios: First, the appearance of a bion state plus a vibrating kink. Second, a single vibrating kink remains after collision. Third, two bion states plus a vibrating kink appear after collision. Forth, the reappearance of the triad $K\bar{K}K$ which specifies the scattering windows. However, in the context of the φ^4 system for $v < v_{cr}$, we can also see narrow intervals close to v_{cr} for which the $K\bar{K}K$ reappear after collisions. Otherwise, the $K\bar{K}K$ collision always leads to a single oscillating kink. Near the edge of the scattering windows in the φ^4 system, the appearance of a bion state plus a vibrating kink can occur exceptionally.

Although both φ^4 and periodic φ^4 systems have the same form of potential in the range $-1 \leq \varphi \leq 1$ and have the same kink and antikink solutions, their differences elsewhere (i.e. $\varphi < -1$ and $1 < \varphi$) will cause significant changes in the interactive features. Hence, we can call the form of potential elsewhere *interaction potential*". This idea can be used to introduce any other type of φ^4 systems with different interaction potential forms. For example, one can study a modified φ^4 system with a interaction potential in the following

form:

$$V(\varphi) = \frac{1}{2}B(\varphi^2 - 1)^2, \quad \varphi < -1 \quad \text{and} \quad 1 < \varphi, \quad (27)$$

where B can be any arbitrary positive number. It is undeniable that the case $B = 1$ is the same ordinary φ^4 system. Many interesting features, such as v_{cr} , can be obtained as a function of the parameter B . Furthermore, one can study the well-known SG system with different interaction potential forms as well.

References

- [1] Vilenkin, A., & Shellard, E. P. S. (2000). *Cosmic strings and other topological defects*. Cambridge University Press.
- [2] Manton, N., & Sutcliffe, P. (2004). *Topological solitons*. Cambridge University Press.
- [3] Ahlqvist, P., Eckerle, K., & Greene, B. (2015). *Kink collisions in curved field space*. Journal of high energy physics, **2015(4)**, 59.
- [4] Greenwood, E., Halstead, E., Poltis, R., & Stojkovic, D. (2009). *Electroweak vacua, collider phenomenology, and possible connection with dark energy*. Physical Review D, **79(10)**, 103003.
- [5] Alfimov, G. L., Malishevskii, A. S., & Medvedeva, E. V. (2014). *Discrete set of kink velocities in Josephson structures: The nonlocal double sineGordon model*. Physica D: Nonlinear Phenomena, **282**, 16-26.
- [6] Bishop, A. R., Krumhansl, J. A., & Trullinger, S. E. (1980). *Solitons in condensed matter: a paradigm*. Physica D: Nonlinear Phenomena, **1(1)**, 1-44.
- [7] DeWolfe, O., Freedman, D. Z., Gubser, S. S., & Karch, A. (2000). *Modeling the fifth dimension with scalars and gravity*. Physical Review D, **62(4)**, 046008.
- [8] Peyravi, M., Riazi, N., & Lobo, F. S. (2016). *Soliton models for thick branes*. The European Physical Journal C, **76(5)**, 247.
- [9] Hawking, S. W., Moss, I. G., & Stewart, J. M. (1982). *Bubble collisions in the very early universe*. Physical Review D, **26(10)**, 2681.
- [10] Giblin Jr, J. T., Hui, L., Lim, E. A., & Yang, I. S. (2010). *How to run through walls: dynamics of bubble and soliton collisions*. Physical Review D, **82(4)**, 045019.
- [11] Gani, V. A., Lizunova, M. A., & Radomskiy, R. V. (2016). *Scalar triplet on a domain wall: an exact solution*. Journal of High Energy Physics, **2016(4)**, 43.
- [12] Peyravi, M., Riazi, N., & Lobo, F. S. (2017). *Evolution of spherical domain walls in solitonic symmetron models*. Physical Review D, **95(6)**, 064047.
- [13] Kobayashi, M., & Nitta, M. (2013). *Sine-Gordon kinks on a domain wall ring*. Physical Review D, **87(8)**, 085003.
- [14] Morris, J. R. (2019). *Interacting kinks and meson mixing*. Annals of Physics, **400**, 346-365.
- [15] Gani, V. A., Kirillov, A. A., & Rubin, S. G. (2018). *Classical transitions with the topological number changing in the early Universe*. Journal of Cosmology and Astroparticle Physics, **2018(04)**, 042.
- [16] Lensky, V. A., Gani, V. A., & Kudryavtsev, A. E. (2001). *Domain walls carrying a U(1) charge*. Journal of Experimental and Theoretical Physics, **93(4)**, 677-684.

- [17] Bazeia, D., Losano, L., & Santos, J. R. L. (2013). *Kinklike structures in scalar field theories: from one-field to two-field models*. Physics Letters A, **377** (25-27), 1615-1620.
- [18] Alonso-Izquierdo, A. (2018). *Kink dynamics in a system of two coupled scalar fields in two spacetime dimensions*. Physica D: Nonlinear Phenomena, **365**, 12-26
- [19] Alonso-Izquierdo, A. (2018). *Reflection, transmutation, annihilation, and resonance in two-component kink collisions*. Physical Review D, **97**(4), 045016.
- [20] Katsura, H. (2014). *Composite-kink solutions of coupled nonlinear wave equations*. Physical Review D, *89*(8), 085019.
- [21] Correa, R. A. C., de Souza Dutra, A., & Gleiser, M. (2014). *Information-entropic measure of energy-degenerate kinks in two-field models*. Physics Letters B, **737**, 388-394.
- [22] Bazeia, D., Lobao, A. S., Losano, L., & Menezes, R. (2014). *First-order formalism for twinlike models with several real scalar fields*. The European Physical Journal C, **74**(2), 2755.
- [23] Mohammadi, M., & Riazi, N. (2019). *The affective factors on the uncertainty in the collisions of the soliton solutions of the double field sine-Gordon system*. Communications in Nonlinear Science and Numerical Simulation, **72**, 176-193.
- [24] Riazi, N., Azizi, A., & Zebarjad, S. M. (2002). *Soliton decay in a coupled system of scalar fields*. Physical Review D, **66**(6), 065003.
- [25] Gani, V. A., & Kudryavtsev, A. E. (2001). *Collisions of domain walls in a supersymmetric model*. Physics of Atomic Nuclei, **64**(11), 2043-2050.
- [26] Gani, V. A., Ksenzov, V. G., & Kudryavtsev, A. E. (2010). *Example of a self-consistent solution for a fermion on domain wall*. Physics of Atomic Nuclei, **73**(11), 1889-1892.
- [27] Gani, V. A., Ksenzov, V. G., & Kudryavtsev, A. E. (2011). *Stable branches of a solution for a fermion on domain wall*. Physics of Atomic Nuclei, **74**(5), 771-777.
- [28] Gani, V. A., Konyukhova, N. B. , Kurochkin, S. V. , & Lensky V. A. (2004). *Study of stability of a charged topological soliton in the system of two interacting scalar fields*. computational mathematics and mathematical physics, **44**, 1968.
- [29] Mohammadi, M., & Riazi, N. (2014). *Bi-dimensional soliton-like solutions of the nonlinear complex sine-Gordon system*. Progress of Theoretical and experimental Physics, **2014**(2), 023A03.
- [30] Rajaraman, R. (1982). *Solitons and instantons*. North Holland, Elsevier, Amsterdam.
- [31] Campbell, D. K., Schonfeld, J. F., & Wingate, C. A. (1983). *Resonance structure in kink-antikink interactions in φ^4 theory*. Physica D: Nonlinear Phenomena, **9**(1-2), 1-32.
- [32] Campbell, D. K., Peyrard, M., & Sodano, P. (1986). *Kink-antikink interactions in the double sine-Gordon equation*. Physica D: Nonlinear Phenomena, **19**(2), 165-205.
- [33] Charkina, O. V., & Bogdan, M. M. (2006). *Internal modes of solitons and near-integrable highly-dispersive nonlinear systems*. Symmetry, integrability and geometry: methods and applications, **2**(0), 47-12.

- [34] Gharaati, A. R., Riazi, N., & Mohebbi, A. F. (2006). *Internal modes of relativistic solitons*. *International Journal of Theoretical Physics*, **45(1)**, 53-63.
- [35] Morris, J. R. (2018). *Small deformations of kinks and walls*. *Annals of Physics*, **393**, 122-131.
- [36] Gani, V. A., & Kudryavtsev, A. E. (1999). *Kink-antikink interactions in the double sine-Gordon equation and the problem of resonance frequencies*. *Physical Review E*, **60(3)**, 3305.
- [37] Popov, C. A. (2005). *Perturbation theory for the double sine-Gordon equation*. *Wave Motion*, **42(4)**, 309-316.
- [38] Peyravi, M., Montakhab, A., Riazi, N., & Gharaati, A. (2009). *Interaction properties of the periodic and step-like solutions of the double-Sine-Gordon equation*. *The European Physical Journal B*, **72(2)**, 269.
- [39] Wazwaz, A. M. (2006). *Compactons, solitons and periodic solutions for some forms of nonlinear Klein-Gordon equations*. *Chaos, Solitons & Fractals*, *28(4)*, 1005-1013.
- [40] Alonso-Izquierdo, A., & Guilarte, J. M. (2012). *On a family of (1 + 1)-dimensional scalar field theory models: kinks, stability, one-loop mass shifts*. *Annals of Physics*, **327(9)**, 2251-2274.
- [41] Gani, V. A., Kudryavtsev, A. E., & Lizunova, M. A. (2014). *Kink interactions in the (1 + 1)-dimensional φ^6 model*. *Physical Review D*, **89(12)**, 125009
- [42] Gani, V. A., Marjaneh, A. M., Askari, A., Belendryasova, E., & Saadatmand, D. (2018). *Scattering of the double sine-Gordon kinks*. *The European Physical Journal C*, **78(4)**, 345.
- [43] Dorey, P., & Romaczukiewicz, T. (2018). *Resonant kinkantikink scattering through quasinormal modes*. *Physics Letters B*, **779**, 117-123.
- [44] Popov, S. P. (2014). *Interactions of breathers and kink pairs of the double sine-Gordon equation*. *Computational Mathematics and Mathematical Physics*, **54(12)**, 1876-1885.
- [45] Bazeia, D., Gomes, A. R., Nobrega, K. Z., & Simas, F. C. (2019). *Kink scattering in a hybrid model*. *Physics Letters B*, *793*, 26-32.
- [46] Khare, A., Christov, I. C., & Saxena, A. (2014). *Successive phase transitions and kink solutions in ϕ^8 , ϕ^{10} , and ϕ^{12} field theories*. *Physical Review E*, **90(2)**, 023208
- [47] Bazeia, D., Belendryasova, E., & Gani, V. A. (2018). *Scattering of kinks of the sinh-deformed φ^4 model*. *The European Physical Journal C*, **78(4)**, 340.
- [48] Goatham, S. W., Mannering, L. E., Hann, R., & Krusch, S. (2011). *Dynamics of Multi-kinks in the Presence of Wells and Barriers*. *Acta Physica Polonica B*, **42**, 2087.
- [49] Popov, S. P. (2013). *Influence of dislocations on kink solutions of the double sine-Gordon equation*. *Computational Mathematics and Mathematical Physics*, **53(12)**, 1891-1899.
- [50] Saadatmand, D., Dmitriev, S. V., Borisov, D. I., & Kevrekidis, P. G. (2014). *Interaction of sine-Gordon kinks and breathers with a parity-time-symmetric defect*. *Physical Review E*, **90(5)**, 052902.

- [51] Saadatmand, D., Dmitriev, S. V., Borisov, D. I., Kevrekidis, P. G., Fatykhov, M. A., & Javidan, K. (2015). *Effect of the ϕ^4 kinks internal mode at scattering on a PT -symmetric defect*. JETP letters, **101(7)**, 497-502.
- [52] Saadatmand, D., Dmitriev, S. V., Borisov, D. I., Kevrekidis, P. G., Fatykhov, M. A., & Javidan, K. (2015). *Kink scattering from a parity-time-symmetric defect in the ϕ^4 model*. Communications in Nonlinear Science and Numerical Simulation, **29(1-3)**, 267-282.
- [53] Fei, Z., Kivshar, Y. S., & Vazquez, L. (1992). *Resonant kink-impurity interactions in the φ^4 model*. Physical Review A, **46(8)**, 5214.
- [54] Fei, Z., Kivshar, Y. S., & Vazquez, L. (1992). *Resonant kink-impurity interactions in the sine-Gordon model*. Physical Review A, **45(8)**, 6019.
- [55] Kivshar, Y. S., Fei, Z., & Vazquez, L. (1991). *Resonant soliton-impurity interactions*. Physical review letters, **67(10)**, 1177.
- [56] Lizunova, M. A., Kager, J., de Lange, S., & van Wezel, J. (2020). *Kinks and realistic impurity models in φ^4 -theory*. arXiv preprint arXiv:2007.04747.
- [57] Christov, I. C., Decker, R. J., Demirkaya, A., Gani, V. A., Kevrekidis, P. G., & Radomskiy, R. V. (2019). *Long-range interactions of kinks*. Physical Review D, **99(1)**, 016010.
- [58] Belendryasova, E., & Gani, V. A. (2019). *Scattering of the φ^8 kinks with power-law asymptotics*. Communications in Nonlinear Science and Numerical Simulation, **67**, 414-426.
- [59] Bazeia, D., Menezes, R., & Moreira, D. C. (2018). *Analytical study of kinklike structures with polynomial tails*. Journal of Physics Communications, **2(5)**, 055019.
- [60] Christov, I. C., Decker, R. J., Demirkaya, A., Gani, V. A., Kevrekidis, P. G., Khare, A., & Saxena, A. (2019). *Kink-kink and kink-antikink interactions with long-range tails*. Physical review letters, **122(17)**, 171601.
- [61] Manton, N. S. (2019). *Forces between kinks and antikinks with long-range tails*. Journal of Physics A: Mathematical and Theoretical, **52(6)**, 065401.
- [62] Christov, I. C., Decker, R. J., Demirkaya, A., Gani, V. A., Kevrekidis, P. G., & Saxena, A. (2020). *Kink-Antikink Collisions and Multi-Bounce Resonance Windows in Higher-Order Field Theories*. arXiv preprint arXiv:2005.00154.
- [63] Gani, V. A., Moradi Marjaneh, A., & Saadatmand, D. (2019). *Multi-kink scattering in the double sine-Gordon model*. The European Physical Journal C, **79(7)**, 620.
- [64] Moradi Marjaneh, A., Saadatmand, D., Zhou, K., Dmitriev, S. V., & Zomorrodian, M. E. (2017). *High energy density in the collision of N kinks in the ϕ^4 model*. Communications in Nonlinear Science and Numerical Simulation, **49**, 30-38.
- [65] Moradi Marjaneh, A., Gani, V. A., Saadatmand, D., Dmitriev, S. V., & Javidan, K. (2017). *Multi-kink collisions in the ϕ^6 model*. Journal of High Energy Physics, **2017(7)**, 28.
- [66] Hassanabadi, H., Lu, L., Maghsoodi, E., Liu, G., & Zarrinkamar, S. (2014). *Scattering of Klein-Gordon particles by a Kink-like potential*. Annals of Physics, **342**, 264-269.
- [67] Takyi, I., & Weigel, H. (2016). *Collective coordinates in one-dimensional soliton models revisited*. Physical Review D, **94(8)**, 085008.

- [68] Baron, H. E., Luchini, G., & Zakrzewski, W. J. (2014). *Collective coordinate approximation to the scattering of solitons in the (1 + 1) dimensional NLS model*. Journal of Physics A: Mathematical and Theoretical, **47(26)**, 265201.
- [69] Javidan, K. (2010). *Collective coordinate variable for soliton-potential system in sine-Gordon model*. Journal of mathematical physics, **51(11)**, 112902.
- [70] Christov, I., & Christov, C. I. (2008). *Physical dynamics of quasi-particles in nonlinear wave equations*. Physics Letters A, **372(6)**, 841-848
- [71] Radomskiy, R. V., Mrozovskaya, E. V., Gani, V. A., & Christov, I. C. (2017). *Topological defects with power-law tails*. In J. Phys. Conf. Ser, **798**, 012087.
- [72] Manton, N. S. (1979). *An effective Lagrangian for solitons*. Nuclear Physics B, **150**, 397-412.
- [73] Kevrekidis, P. G., Khare, A., & Saxena, A. (2004). *Solitary wave interactions in dispersive equations using Manton's approach*. Physical Review E, **70(5)**, 057603.
- [74] Peyrard, M., & Campbell, D. K. (1983). *Kink-antikink interactions in a modified sine-Gordon model*. Physica D: Nonlinear Phenomena, **9(1-2)**, 33-51.
- [75] Goodman, R. H., & Haberman, R. (2005). *Kink-Antikink Collisions in the ϕ^4 Equation: The n -Bounce Resonance and the Separatrix Map*. SIAM Journal on Applied Dynamical Systems, **4(4)**, 1195-1228.
- [76] Charkina, O. V., & Bogdan, M. M. (2006). *Internal modes of solitons and near-integrable highly-dispersive nonlinear systems*. Symmetry, integrability and geometry: methods and applications, **2(0)**, 47-12.
- [77] Kivshar, Y. S., Pelinovsky, D. E., Cretegny, T., & Peyrard, M. (1998). *Internal modes of solitary waves*. Physical review letters, **80(23)**, 5032.
- [78] Mohammadi, M., & Riazi, N. (2011). *Approaching integrability in bi-dimensional nonlinear field equations*. Progress of Theoretical Physics, **126(2)**, 237-248.
- [79] Mohammadi, M., Riazi, N., & Azizi, A. (2012). *Radiative Properties of Kinks in the $\sin^4(\phi)$ System*. Progress of theoretical physics, **128(4)**, 615-627.
- [80] Campbell, D. K., & Peyrard, M. (1986). *Solitary wave collisions revisited*. Physica D: Nonlinear Phenomena, **18(1-3)**, 47-53.
- [81] Belova, T. I., & Kudryavtsev, A. E. (1997). *Solitons and their interactions in classical field theory*. Physics-Uspekhi, **40(4)**, 359.
- [82] Anninos, P., Oliveira, S., & Matzner, R. A. (1991). *Fractal structure in the scalar $\lambda(\varphi^2 - 1)^2$ theory*. Physical Review D, **44(4)**, 1147.
- [83] Goodman, R. H., & Haberman, R. (2007). *Chaotic scattering and the n -bounce resonance in solitary-wave interactions*. Physical review letters, **98(10)**, 104103.
- [84] Gani, V. A., Lensky, V., & Lizunova, M. A. (2015). *Kink excitation spectra in the (1 + 1)-dimensional φ^8 model*. Journal of High Energy Physics, **2015(8)**, 147.
- [85] Quintero, N. R., Snchez, A., & Mertens, F. G. (2000). *Resonances in the dynamics of φ^4 kinks perturbed by ac forces*. Physical Review E, **62(4)**, 5695.
- [86] Alonso-Izquierdo, A., Nieto, L. M., & Queiroga-Nunes, J. (2020). *Scattering between wobbling kinks*. arXiv preprint arXiv:2007.15517.

- [87] Fei, Z., Konotop, V. V., Peyrard, M., & Vazquez, L. (1993). *Kink dynamics in the periodically modulated φ^4 model*. Physical Review E, **48(1)**, 548.
- [88] Azizi, A., & Mohammadi, M. (2010). *Separability in 1+ 1 Dimensions in Classical Nonlinear Fields*. arXiv preprint arXiv:1004.4780.
- [89] Derrick, G. H. (1964). *Comments on nonlinear wave equations as models for elementary particles*. Journal of Mathematical Physics, **5(9)**, 1252-1254.